

# Nanostructured Semiconductor Crystals

## -- Building Blocks for Solar Cells: Shapes, Syntheses, Surface Chemistry, Quantum Confinement Effects

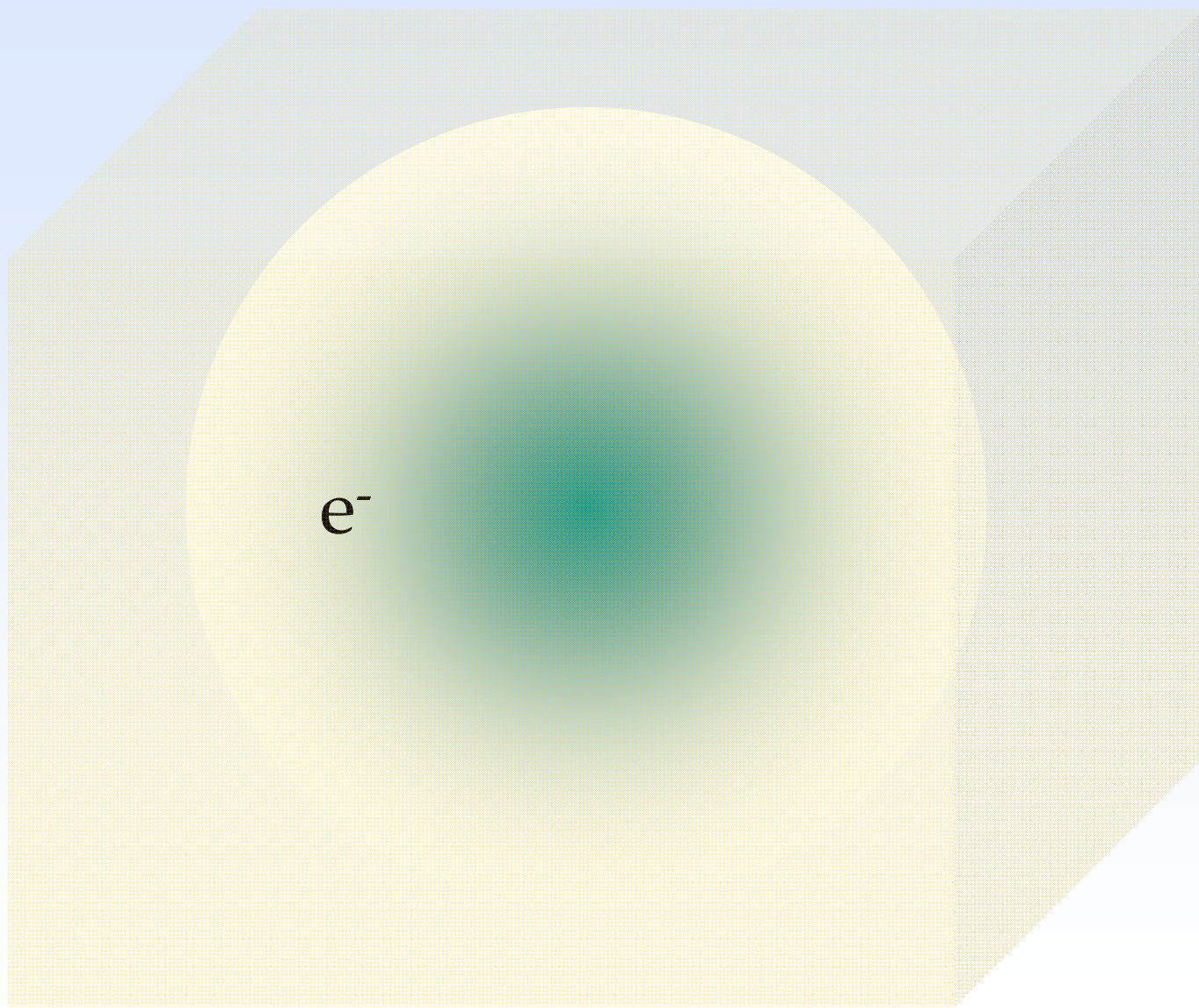
April 12, 2012

The University of Toledo, Department of Physics and Astronomy  
SSARE, PVIC

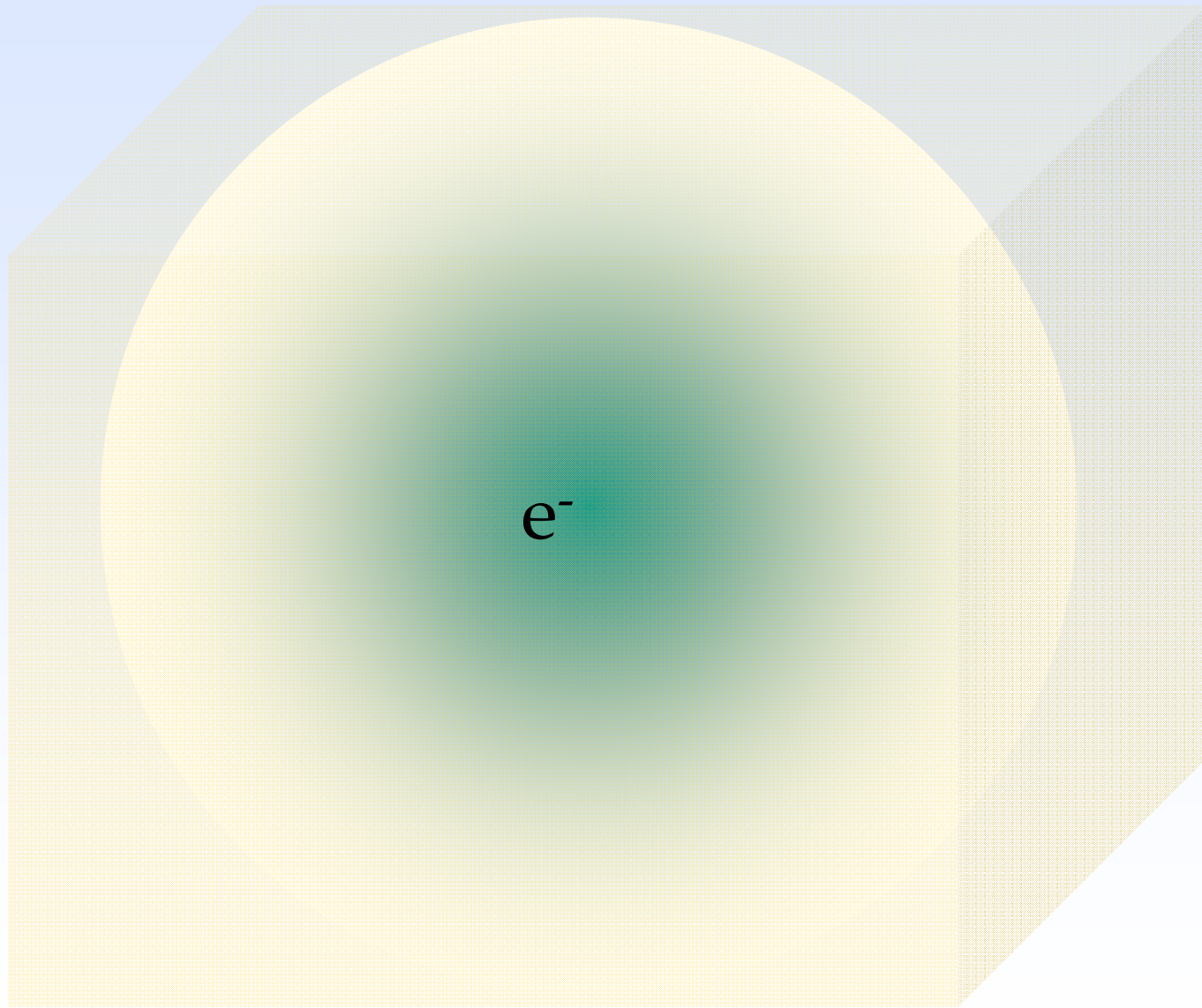
Principles and Varieties of Solar Energy (PHYS 4400)  
and  
Fundamentals of Solar Cells (PHYS 6980)



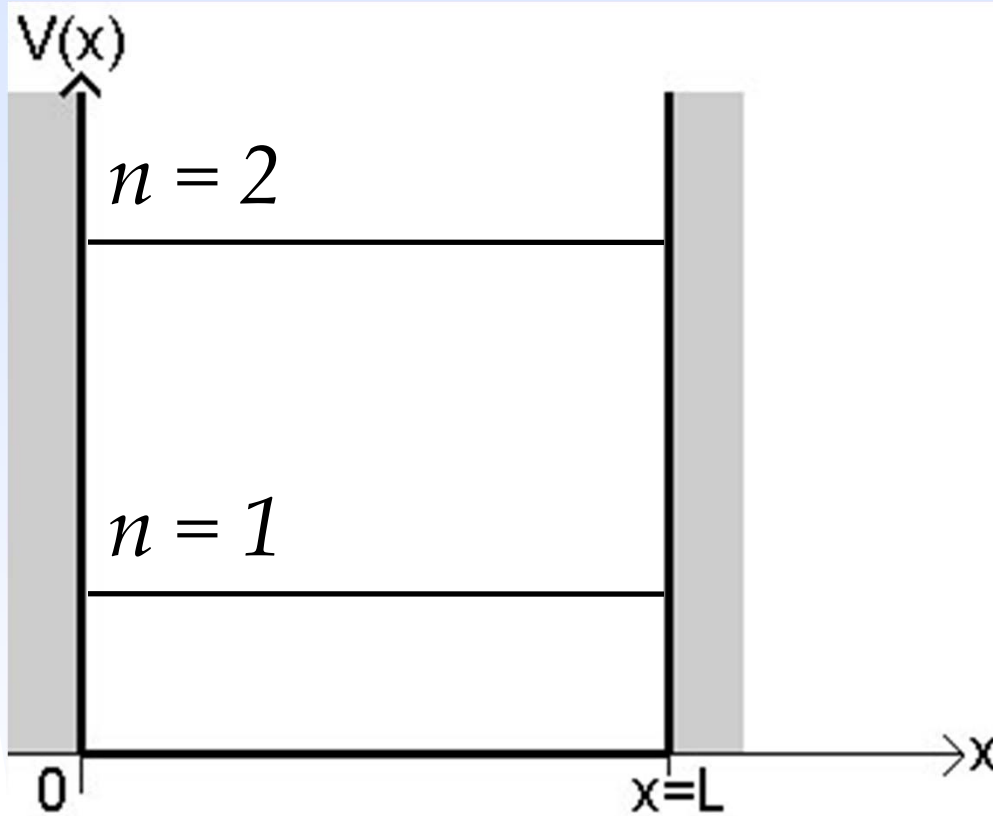
# Quantum confinement effect



## Quantum confinement effect (2)



## Particle in a box (quantum well)




$$E_n = \frac{\hbar^2 \pi^2}{2mL^2} n^2$$

The Potential,  $V(x)$ , is 0 inside the box, and infinite elsewhere (infinite barriers)



## Nanomaterials for solar energy conversion

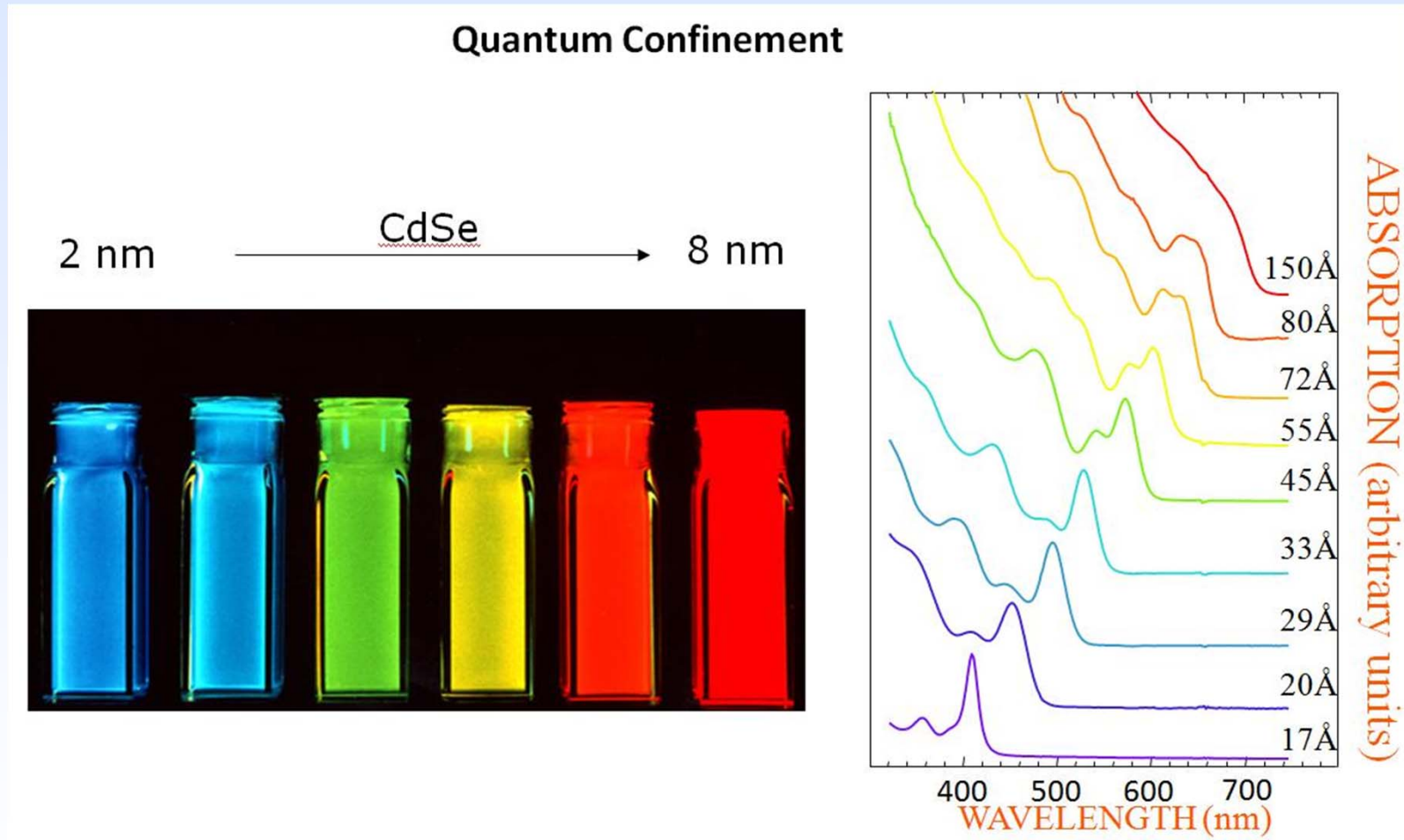
- Enable high surface area devices →
  - strong light absorption (dye-sensitized nanostructured TiO<sub>2</sub>)
  - facilitates fast charge separation (proximity of photoexcited carriers to charge-separating interface)
- Customizable properties enable unique designs →
  - Engineerable (size-dependent) absorption spectrum
  - Varying geometries – e.g., efficient charge transport in quantum rods, nanotubes
  - Controlled chemical functionalization to direct charge separation
- Efficient multiple exciton generation 

# Consequences of Quantization

- *Dramatic variation of optical and electronic properties*
- *Large blue shift of absorption edge*
- *Discrete energy levels/structured absorption and photoluminescence spectra*
- *Enhanced photoredox properties for photogenerated electrons and holes*
- *Enhanced Inverse Auger (impact ionization, or multiple exciton generation)*
- *Slowed relaxation and cooling of photogenerated hot electrons and holes (controversial)*
- *PL blinking in single QDs*
- *Conversion of indirect semiconductors to direct semiconductors or vice versa*
- *Greatly enhanced non-linear optical properties*
- *Greatly modified pressure dependence of phase changes and direct to indirect transitions*
- *Efficient anti-Stokes luminescence*



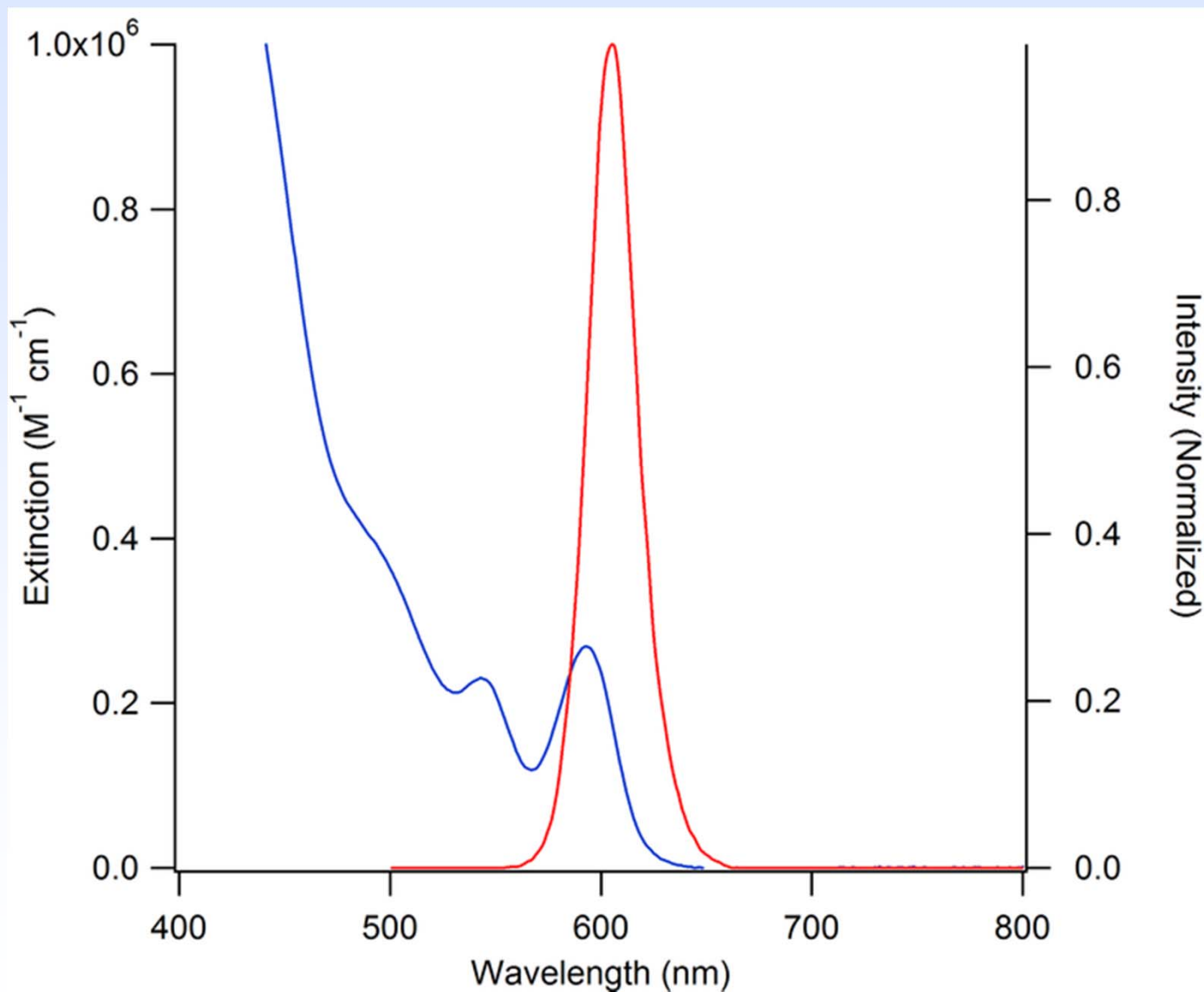
# Size-dependent optical properties



<http://nanocluster.mit.edu/research.php>



## Absorption and emission (CdSe nanocrystals)

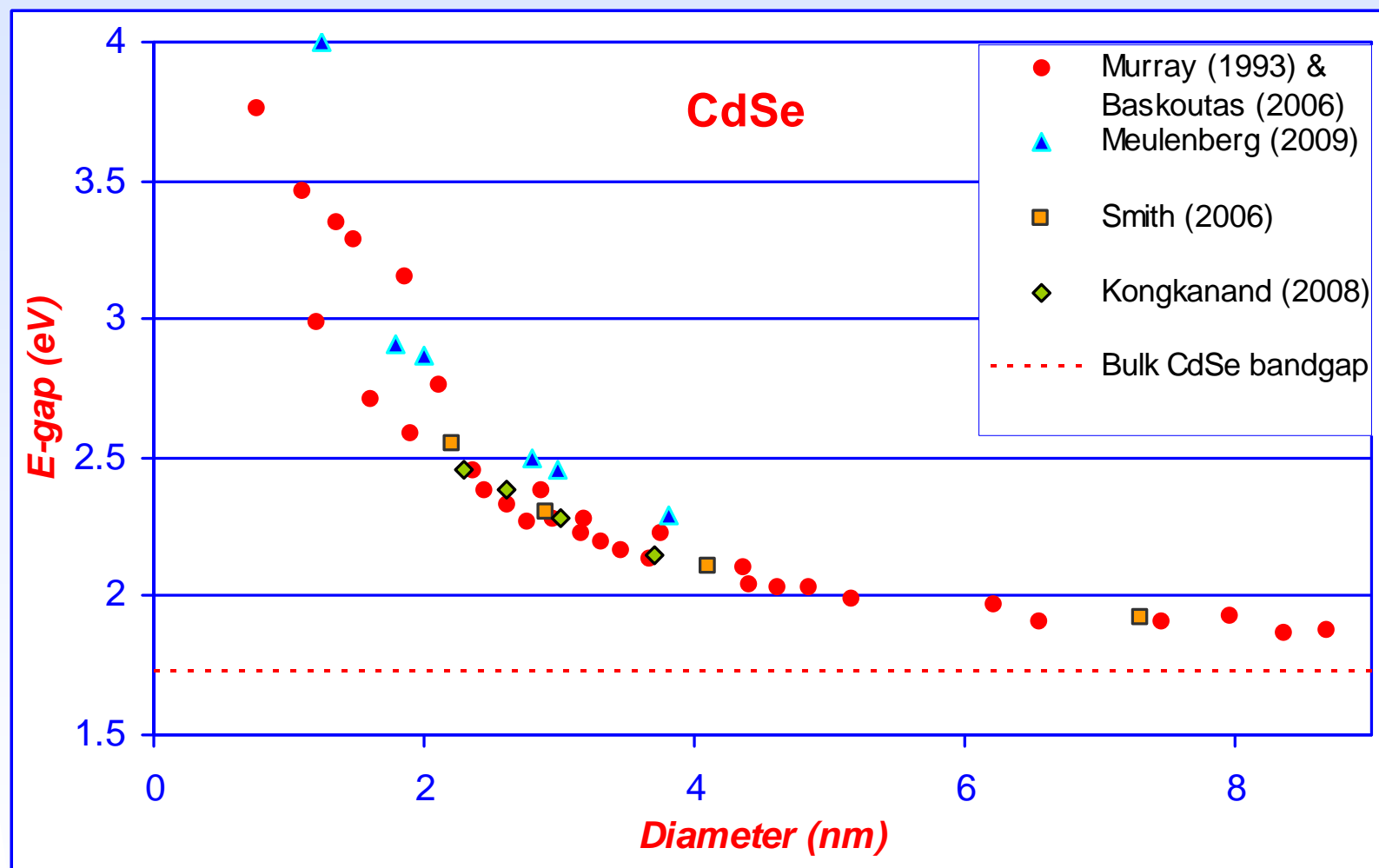


[http://en.wikipedia.org/wiki/File:EF\\_605\\_spectra.png](http://en.wikipedia.org/wiki/File:EF_605_spectra.png)





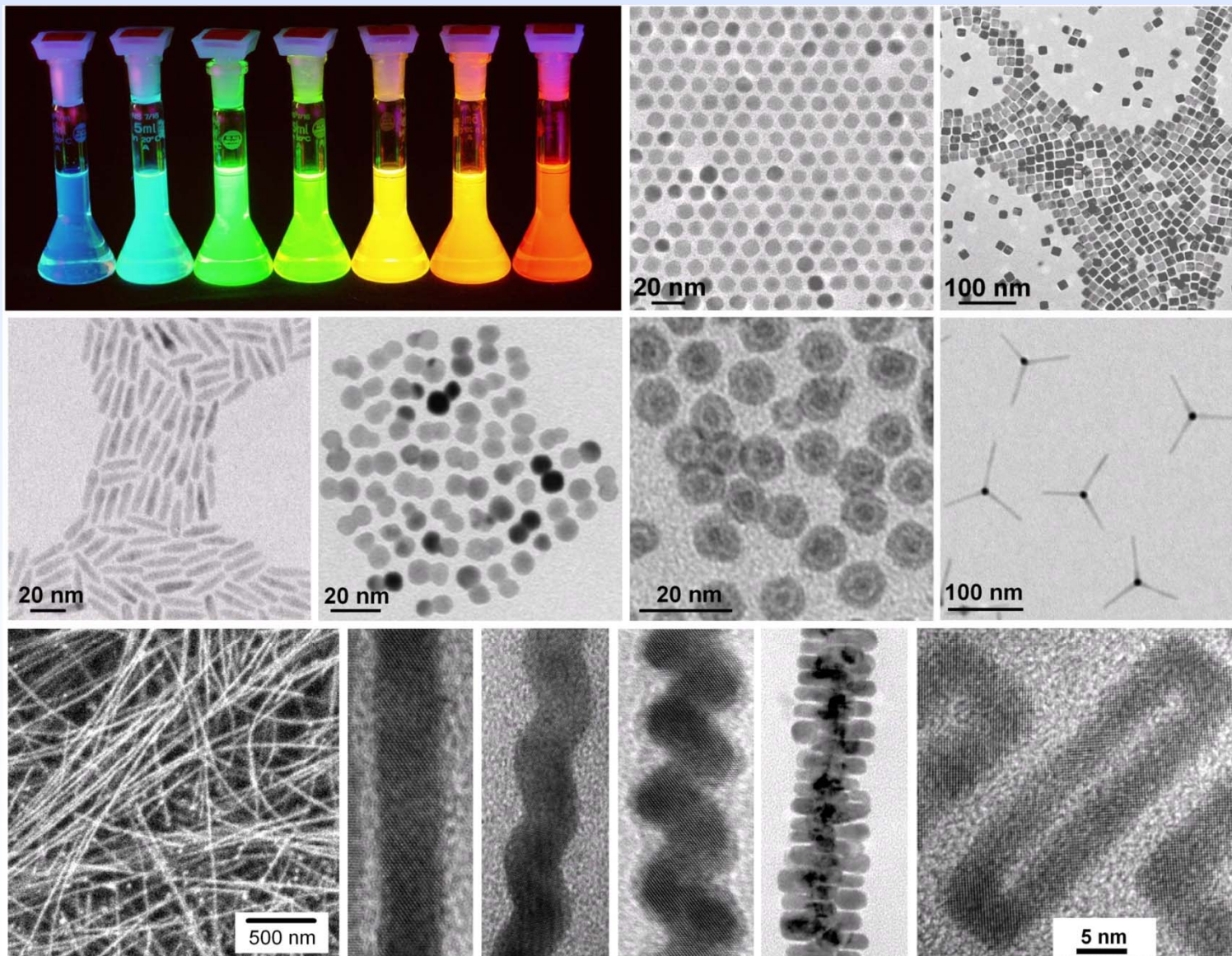
## Size-dependent bandgap of CdSe NCs



From "Physical and Optical Properties of Colloidal Semiconducting Nanocrystals for Solar Absorption", by Abdel Ibdah (UT)



# Colloidal nanostructures (crystalline)



<http://talapinlab.uchicago.edu>

.... energizing Ohio for the 21st Century



## Quantum Confined Structures – Density of States

The number of states between  $k$  and  $k + dk$  in 3, 2, and 1 dimensions:

$$\frac{dN_{3D}}{dk} = 2 \left( \frac{L}{2\pi} \right)^3 4\pi k^2, \quad \frac{dN_{2D}}{dk} = 2 \left( \frac{L}{2\pi} \right)^2 2\pi k, \quad \frac{dN_{1D}}{dk} = 2 \left( \frac{L}{2\pi} \right)$$

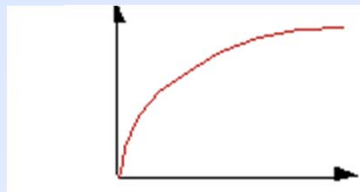
$$g_{c,3D} = \frac{8\pi\sqrt{2}}{h^3} m_{eff}^{3/2} \sqrt{E - E_{min}}$$

$$g_{c,2D} = \frac{4\pi m_{eff}}{h^2}$$

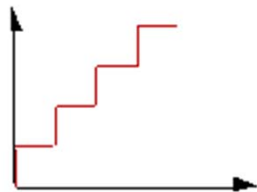
$$g_{c,1D} = \sqrt{\frac{2\pi m_{eff}}{h^2}} \frac{1}{\sqrt{E - E_{min}}}$$



# Quantum confinement effect on density of electronic states

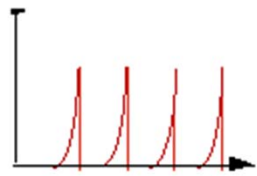


Bulk Semiconductor

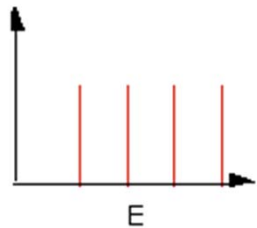


Quantum Well

$N(E)$

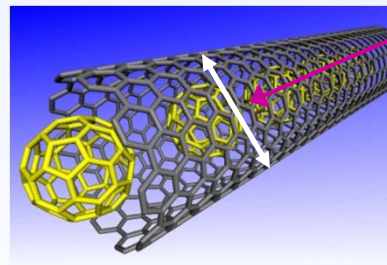
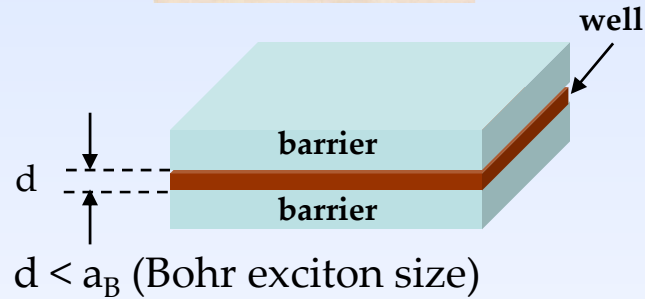


Quantum Wire

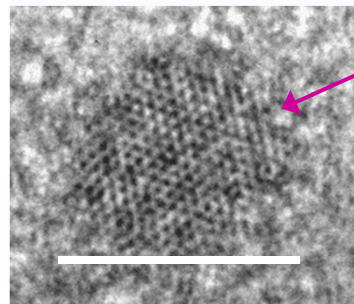


Quantum Dot  
(or Nanocrystal)

$E$



~1 nm



~6 nm dia.

60 Å InP QD

Dimensionality

3D

2D

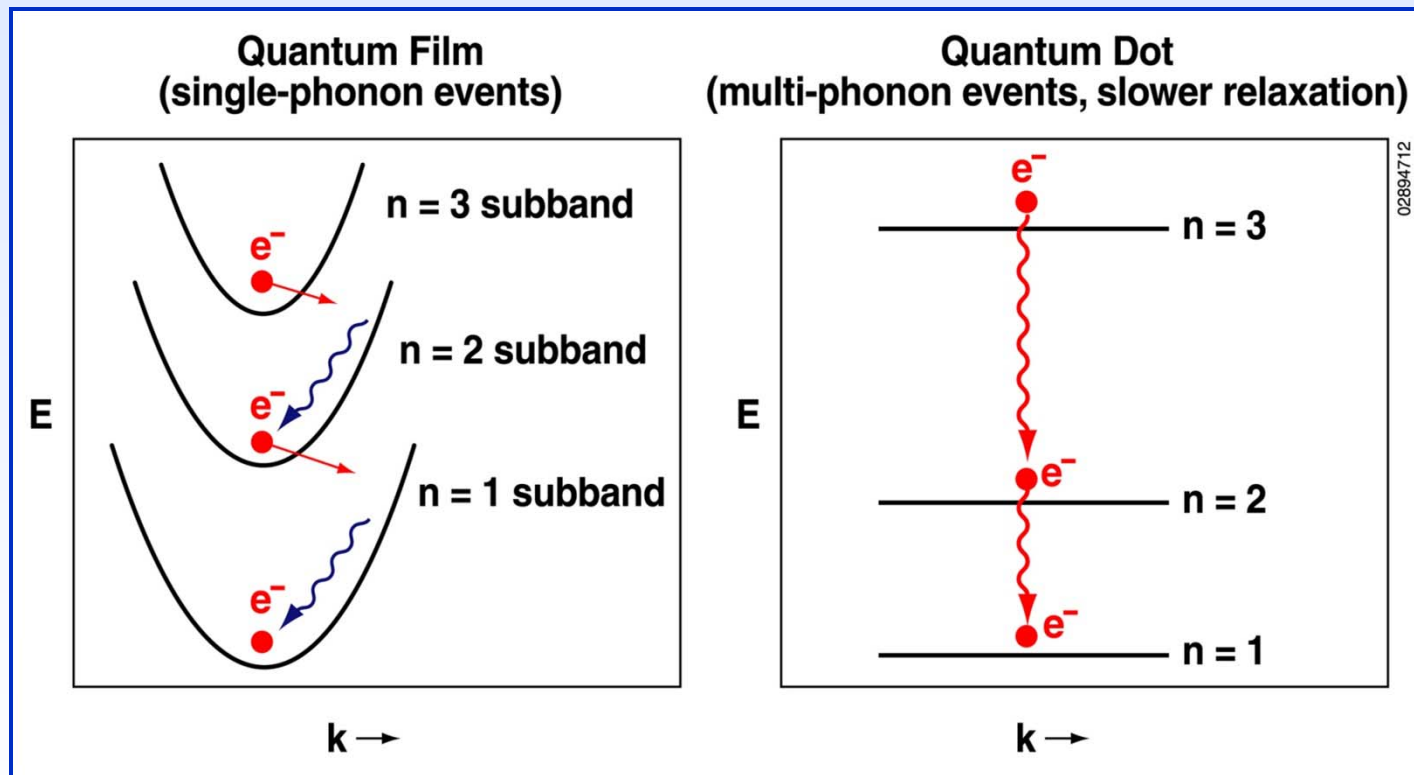
1D

0D



# Hot electron relaxation pathways

## Quantum Films vs Quantum Dots



phonon bottleneck



## Electronic Structure Calculations for 41.8 Å InP QD

Excitonic energies are calculated using the atomistic pseudopotential method (APM). Two steps are involved:

1. single-particle orbital energies and wavefunctions are computed by solving the Schrödinger equation;  $v_\alpha(\mathbf{r} - \mathbf{R}_n - \tau_\alpha)$  is the screened, nonlocal pseudopotential for the atom of type  $\alpha$  located at site  $\tau_\alpha$  in cell  $\mathbf{R}_n$  and  $\epsilon_i$  is the single particle orbital energy.

$$\left\{ -\frac{1}{2}\nabla^2 + \sum_{R_n} \sum_{\tau_\alpha} v_\alpha(\mathbf{r} - \mathbf{R}_n - \tau_\alpha) \right\} \psi_i = \epsilon_i \psi_i$$

2. excitonic energy levels and wavefunctions are calculated using the configuration interaction (CI) approach.



# Calculated energy levels in 42 Å InP QD

## (a) Valence States

### Character of Wavefunction

State Index	Energy (eV)	S	P	D	F
1	-6.0303	76.9	9.5	8.0	1.7
2	-6.0303	76.9	9.5	8.0	1.7
3	-6.0679	2.7	84.9	5.7	2.6
4	-6.0679	2.7	84.9	5.7	2.6
5	-6.1268	0.2	84.2	6.0	4.5
6	-6.1275	69.8	4.8	17.7	2.1
7	-6.1386	2.0	60.5	11.5	16.1
8	-6.1386	2.0	60.5	11.5	16.1
9	-6.1403	0.4	5.3	77.5	5.7
10	-6.1403	0.4	5.3	77.5	5.7
11	-6.1542	0.0	2.9	80.9	4.5
12	-6.1834	40.2	4.2	37.4	3.6
13	-6.1835	40.2	4.1	37.3	3.7
14	-6.1961	0.5	2.2	0.7	82.5
15	-6.2261	37.3	2.1	33.4	5.8
16	-6.2473	0.9	25.4	11	36.9
17	-6.2496	3.0	21.8	14.8	35.2
18	-6.2544	5.1	21.3	7.2	47.3
19	-6.2549	3.5	23.1	16.5	36.4
20	-6.2552	1.9	25.9	18.8	27.5
21	-6.2641	2.0	35.8	21.1	21.1
22	-6.2657	1.5	33.1	14.6	30.5
23	-6.2665	5.3	38.3	8.6	29.1
24	-6.2880	1.6	32.7	15.2	19.3
25	-6.2852	1.9	26.1	20.4	20.9

## (b) Conduction States

### Character of Wavefunction

State Index	Energy (eV)	S	P	D	F
1	-4.0608	82.5	10.6	1.5	1.4
2	-3.7855	5.7	73.2	10.5	2.6
3	-3.7855	5.7	73.2	10.5	2.6
4	-3.7771	5.3	73.1	10.5	2.9
5	-3.7019	0.8	1.2	6.3	0.8
6	-3.7017	0.7	1.1	6.4	0.8
7	-3.7017	0.7	1.1	6.4	0.8
8	-3.6994	2.7	0.3	3.7	0.8
9	-3.6324	1.3	3.3	1.3	16.5
10	-3.6312	0.1	6.1	1.0	9.6
11	-3.6298	0.1	6.3	0.9	9.3
12	-3.6298	0.1	6.3	0.9	9.3
13	-3.5879	4.6	0.9	5.6	5.0
14	-3.5599	1.9	9.0	58.5	12
15	-3.5568	1.8	5.7	39.1	7.5
16	-3.5540	1.6	2.6	22.3	3.9

Valence (a) and conduction (b) single-particle states for a 41.8 Å diameter InP quantum dot. Columns 3-6 indicate the percentage distribution of envelope angular momentum components for each single-particle level. Energies are relative to vacuum.



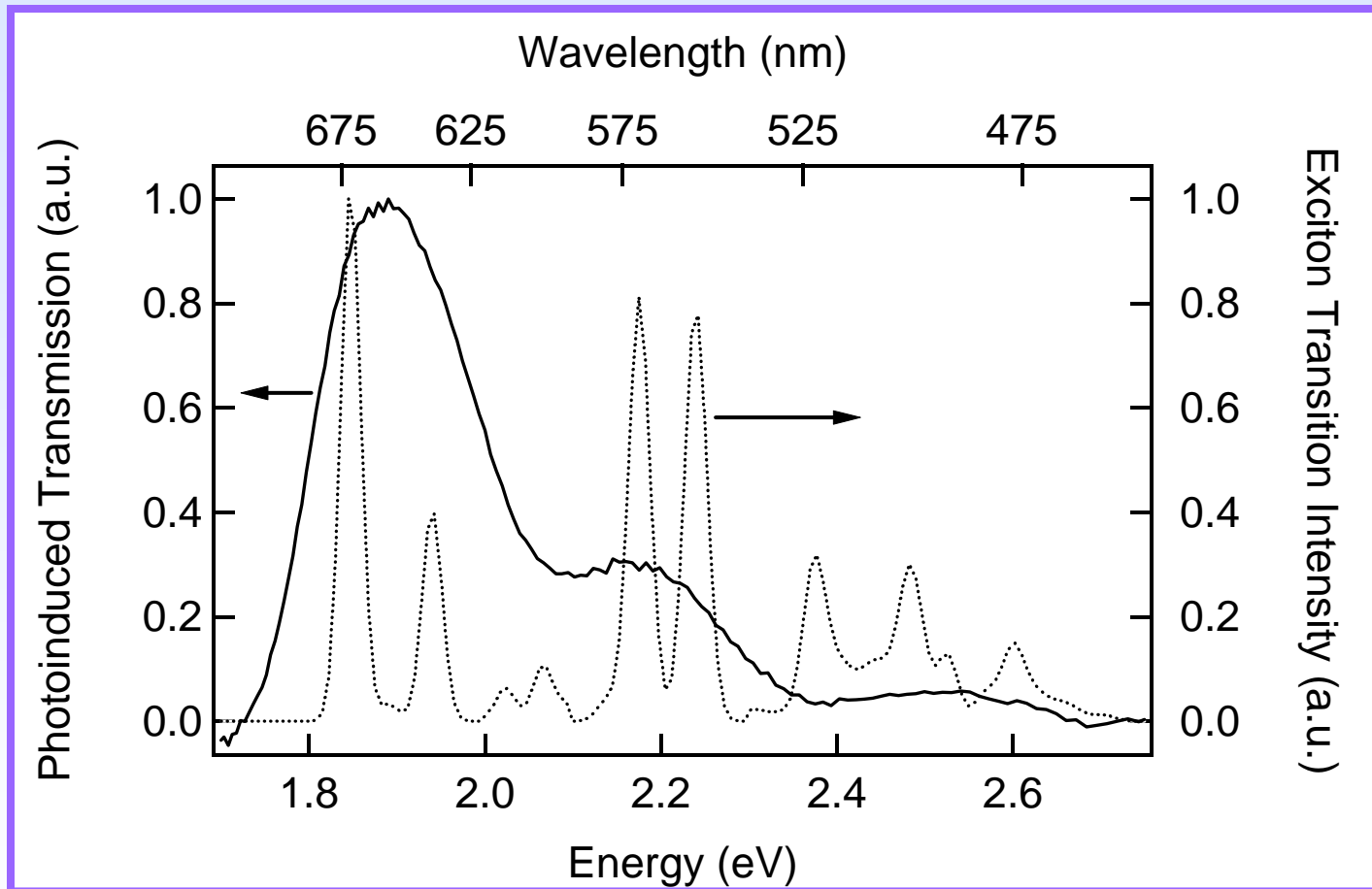
## Calculated *excitonic* transitions in 42 Å InP QD

PEAK POSITION (EV)	INITIAL VALENCE STATES	FINAL CONDUCTION STATES
1.84	1, 2	1
1.94	6	1
2.18	3, 4	2, 3, 4
2.24	5	4
2.24	7, 8	2, 3
2.38	17-25	2, 3, 4
2.48	9, 10, 11	14, 15
2.60	17, 19, 21, 22, 24, 25	14



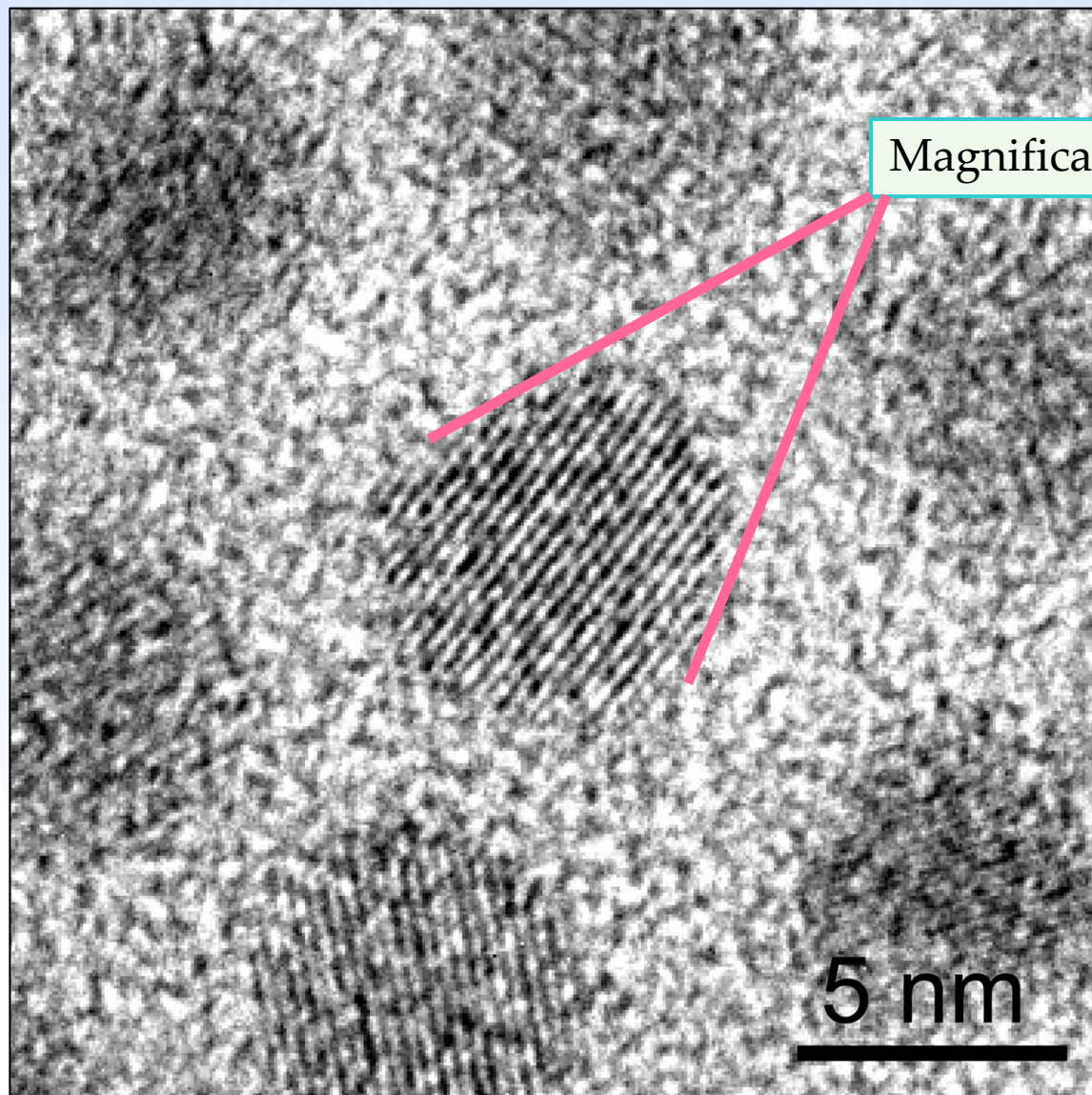


## Excitonic spectrum for 42 Å InP QD



Theoretical excitonic spectrum (dashed line) for a sample of 41.8 Å diameter InP quantum dots. The transition intensity is proportional to the absorption coefficient, and consists of a sum of the oscillator strengths for various excitonic transitions. The solid line shows the measured photoinduced bleach spectrum, at a delay of 1.0 ps, for a sample with average size of ~42 Å diameter. Theoretical transition peaks correspond to those listed at left. The two small peaks between 2.0 and 2.1 eV originate from transitions between valence states 12, 13, and 15, and conduction state 1.

# Transmission electron micrograph (TEM) of Lead Selenide NCs

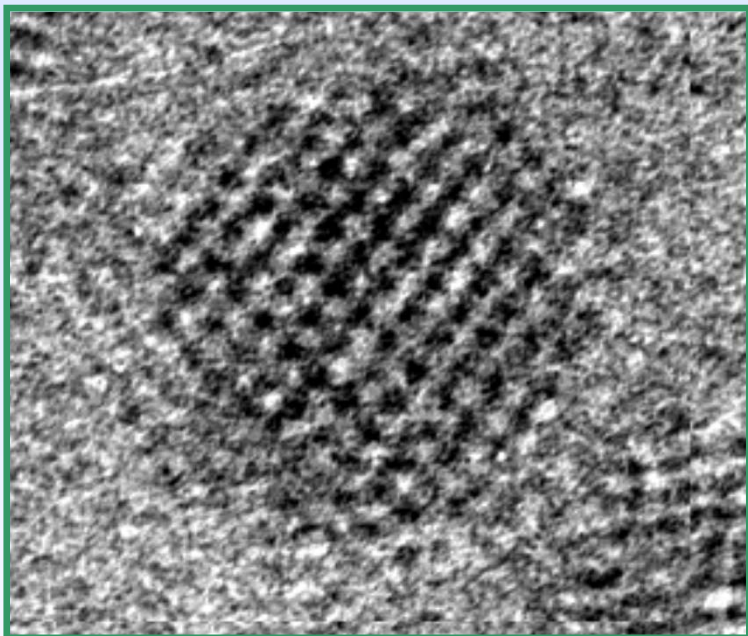


Magnification ~ 2,000,000x

PbSe



# Colloidal quantum dots



TEM image of 60-Å InP QD  
(K.Jones, NREL)

## Colloidal synthesis

InP QDs synthesized by colloidal methods starting with  $\text{InCl}_3$  and tris(trimethylsilyl)phosphine in presence of TOP/TOPO

## Small size – strong confinement regime

small size (15 Å - 80 Å diameter), spherical shape, many confined valence and conduction states [compare to epitaxial SK dots typically  $> 100$  Å, with potential barriers confining  $\sim 6$  conduction and valence states]

## Variable surface chemistry

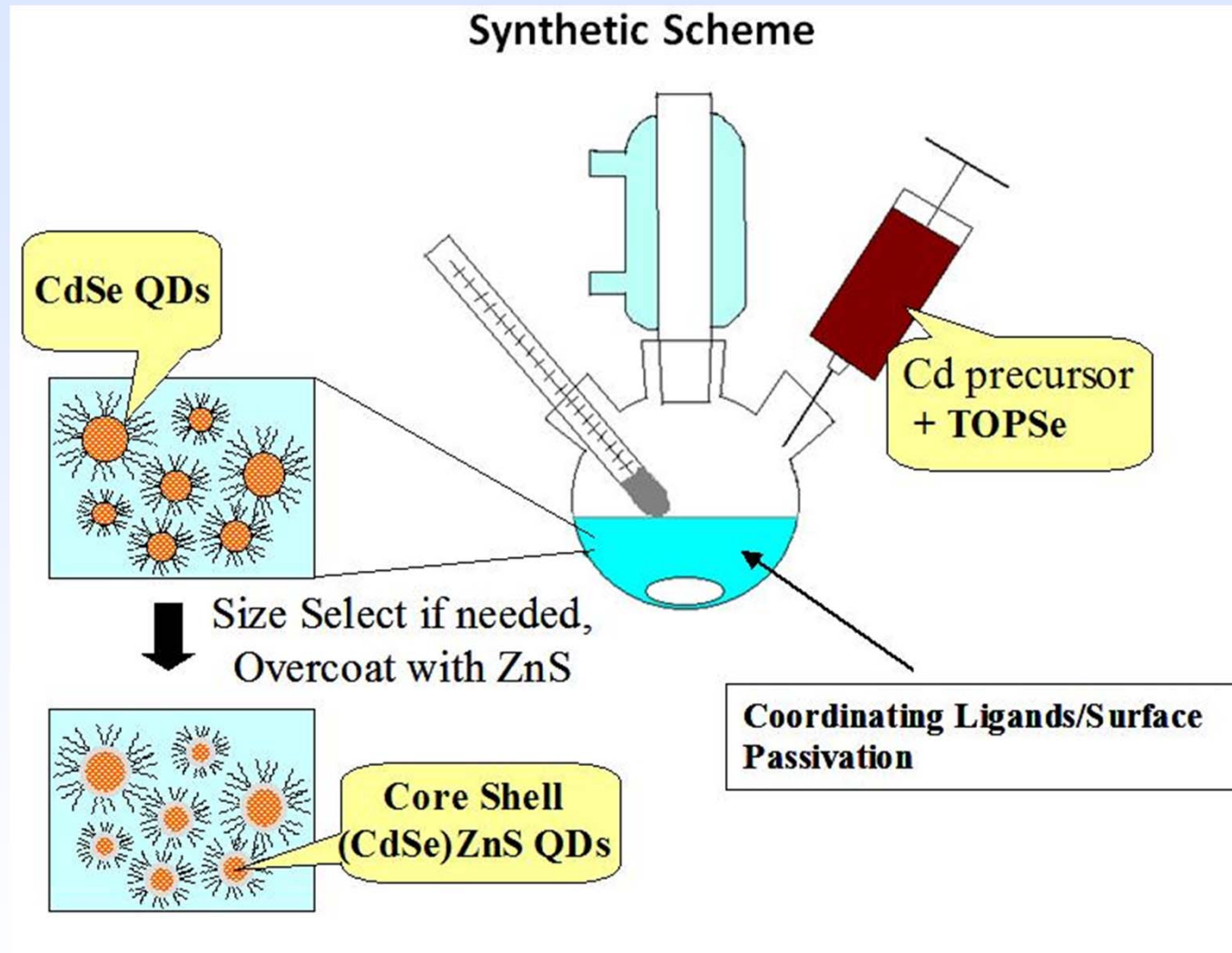
as-prepared dots are capped with organic stabilizer (TOP/TOPO)  $\Rightarrow$  surface chemistry alters electrical and optical (emission) properties (pyridine,  $\text{Na}^+$  - biphenyl<sup>(-)</sup>, etched QDs)

## High ratio of atoms on surface

e.g., for 35 Å dots,  $\sim 30\%$  of atoms reside on surface  $\Rightarrow$  importance of surface effects



# Synthesis of colloidal nanocrystals



<http://nanocluster.mit.edu/research.php>



## Synthesis of colloidal nanocrystals

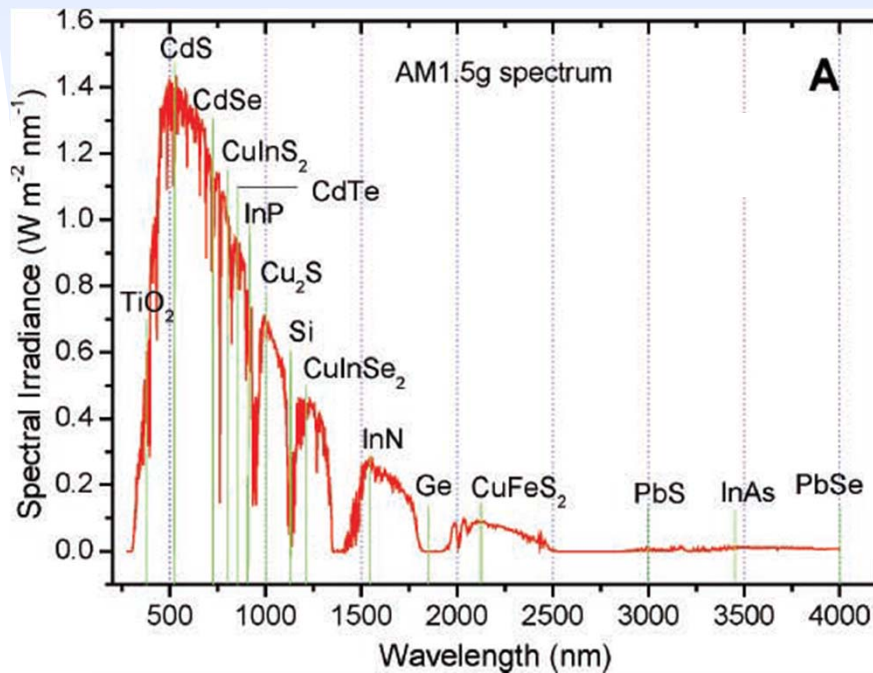


Typical three-headed flask set up. The middle head is connected to the Schlenk line's glass manifold. The left head is covered with a septum pierced by the thermocouple. The right head is for injection. Photo and caption courtesy of T. Kinner (UT).

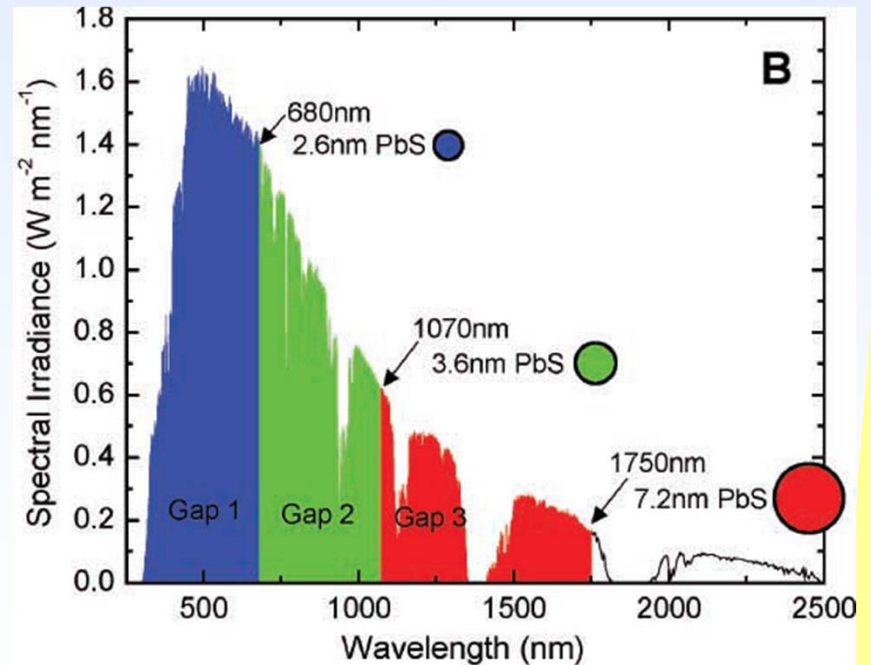


# Why pursue QD solar cells?

1. Colloidal synthesis produces high-quality nanocrystals
2. Solution processed, tunable band-gap
3. Potentially easy to process (**room temperature, ambient air**)
4. Scientifically interesting: balance quantum confinement w/ transport
5. Flexibility (?)



AM1.5G solar spectrum along with some common bulk semiconductors band-gaps



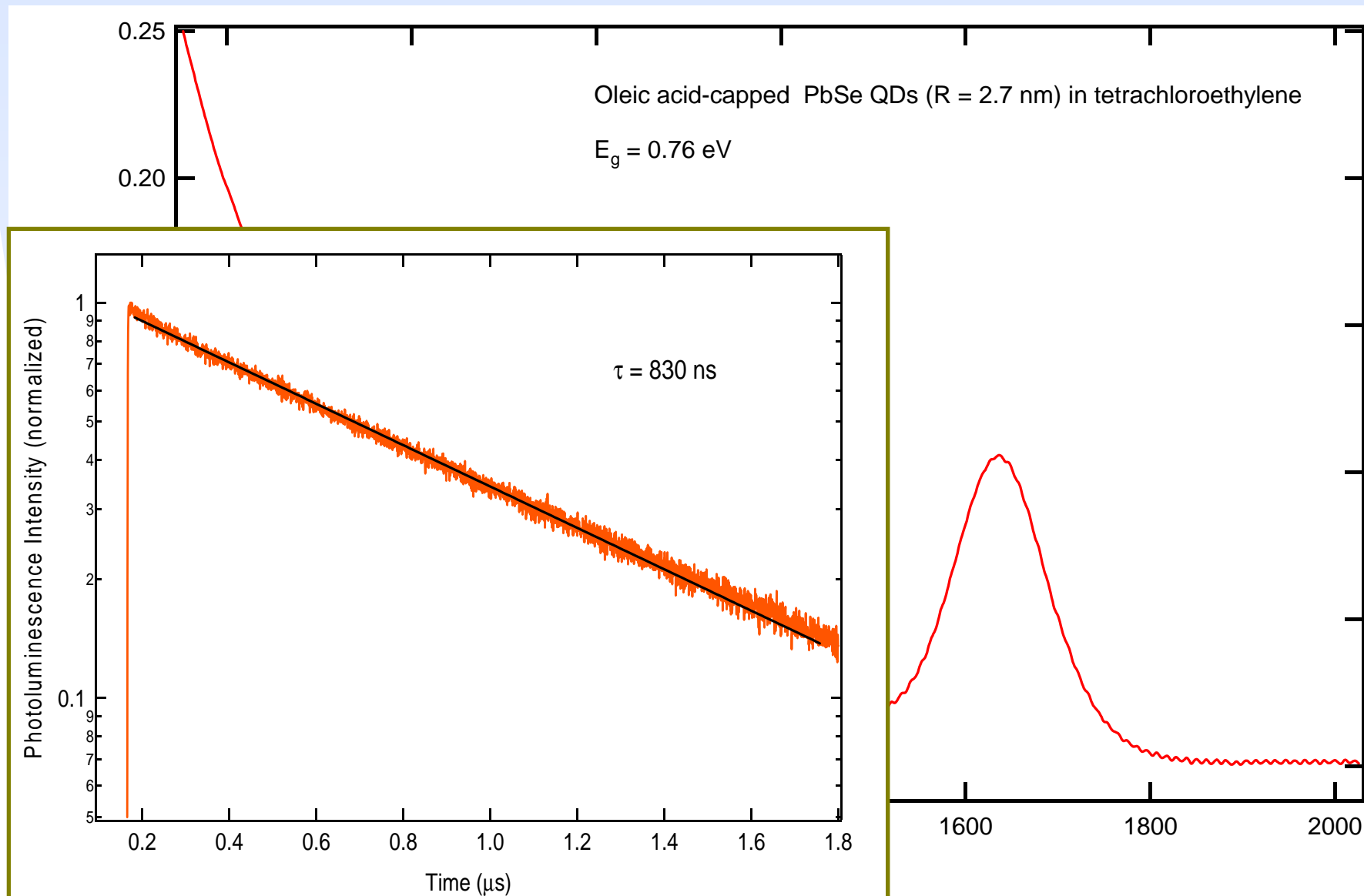
Triple junction PbS dot size

J. Tang, et al., *Adv. Mater.* 22,1(2010)

.... energizing Ohio for the 21st Century



# Colloidal PbSe QDs in tetrachloroethylene (TCE)

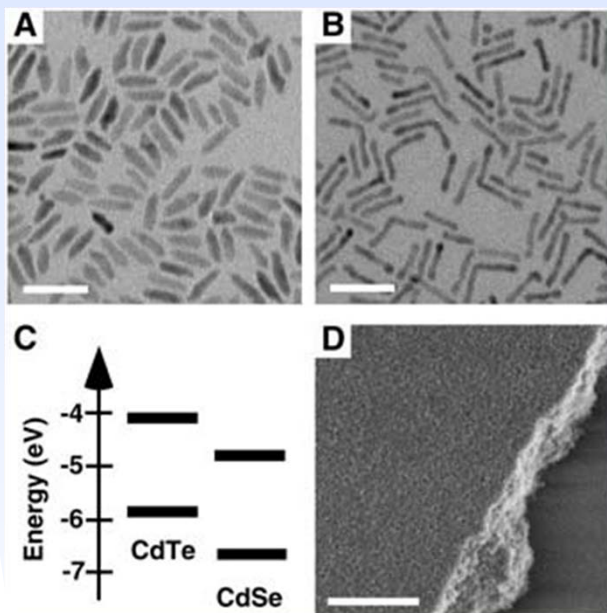


# Annealed NC-based solar cell

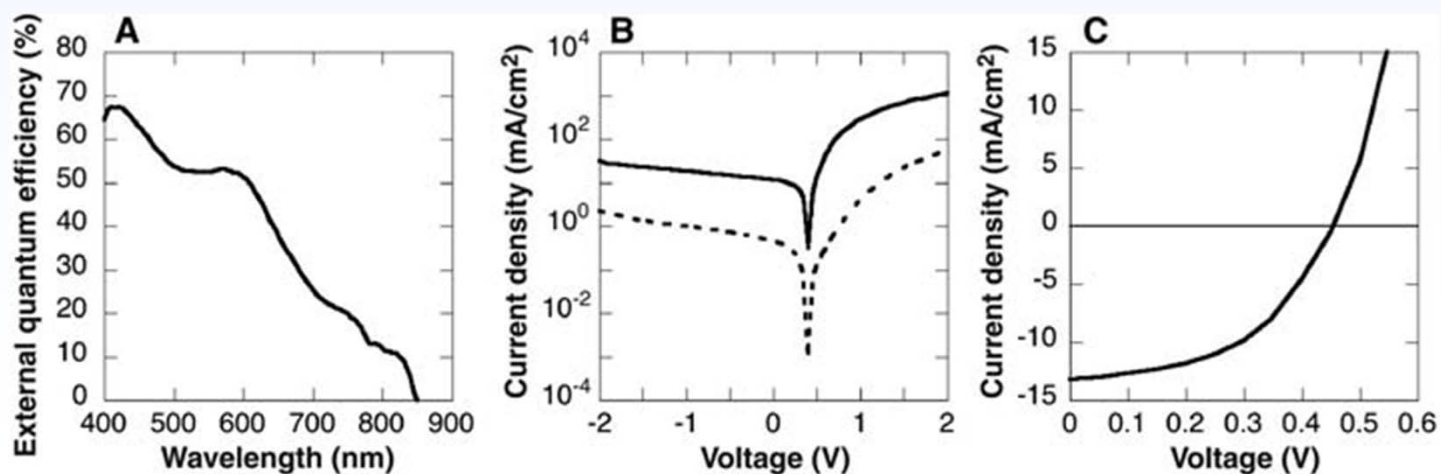
## *Air-Stable All-Inorganic Nanocrystal Solar Cells Processed from Solution*

Ilan Gur, Neil A. Fromer, Michael L. Geier, A. Paul Alivisatos

21 OCTOBER 2005 VOL 310 SCIENCE

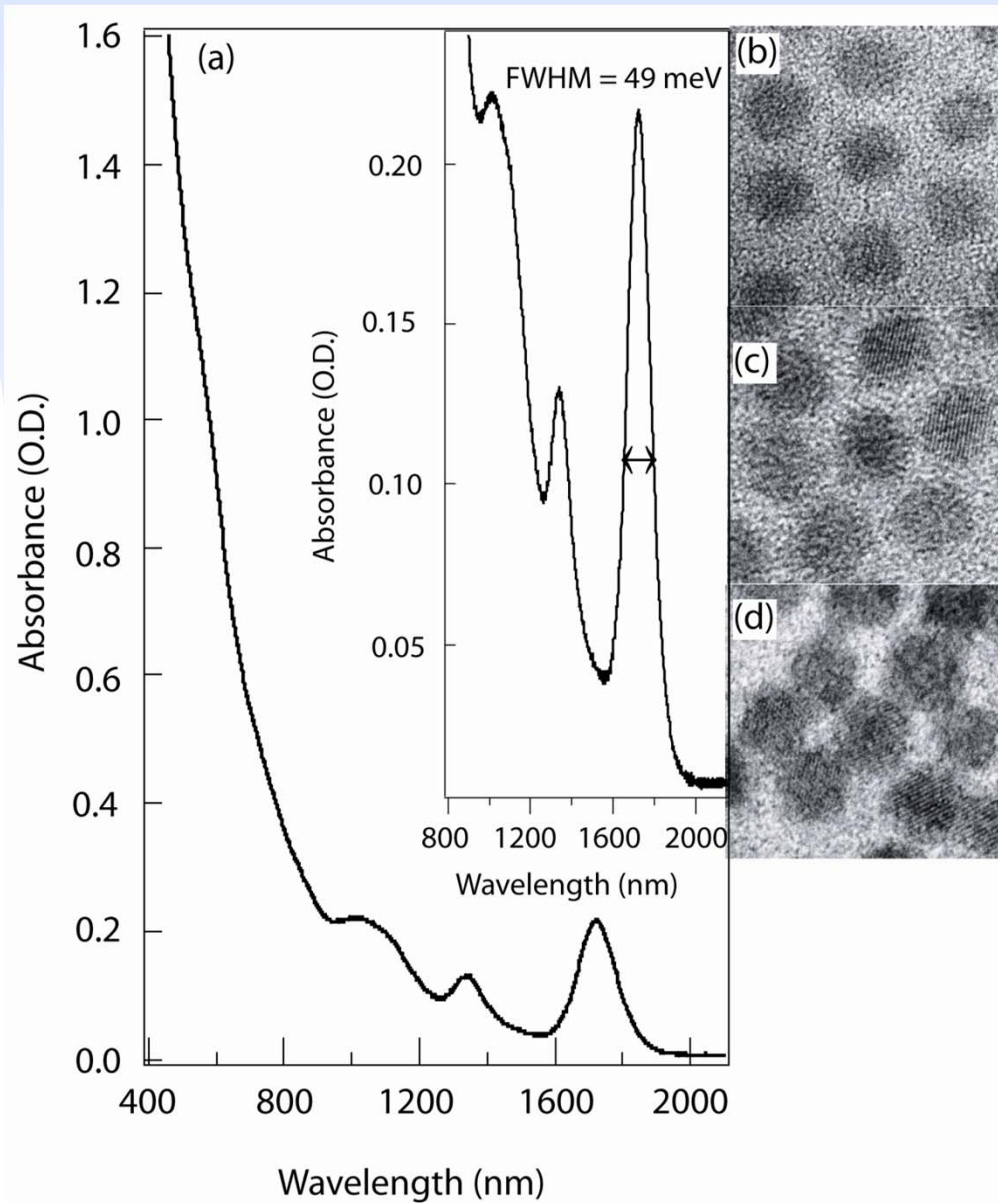


Transmission electron micrographs of (A) CdSe and (B) CdTe NCs used in this investigation. Scale bar, 40 nm. (C) An energy diagram of valence and conduction band levels for CdTe and CdSe illustrates the type II charge-transfer junction formed between the two materials...





## Drop-cast films of 5.7 nm dia. PbSe NCs



oleic acid (1.8 nm)

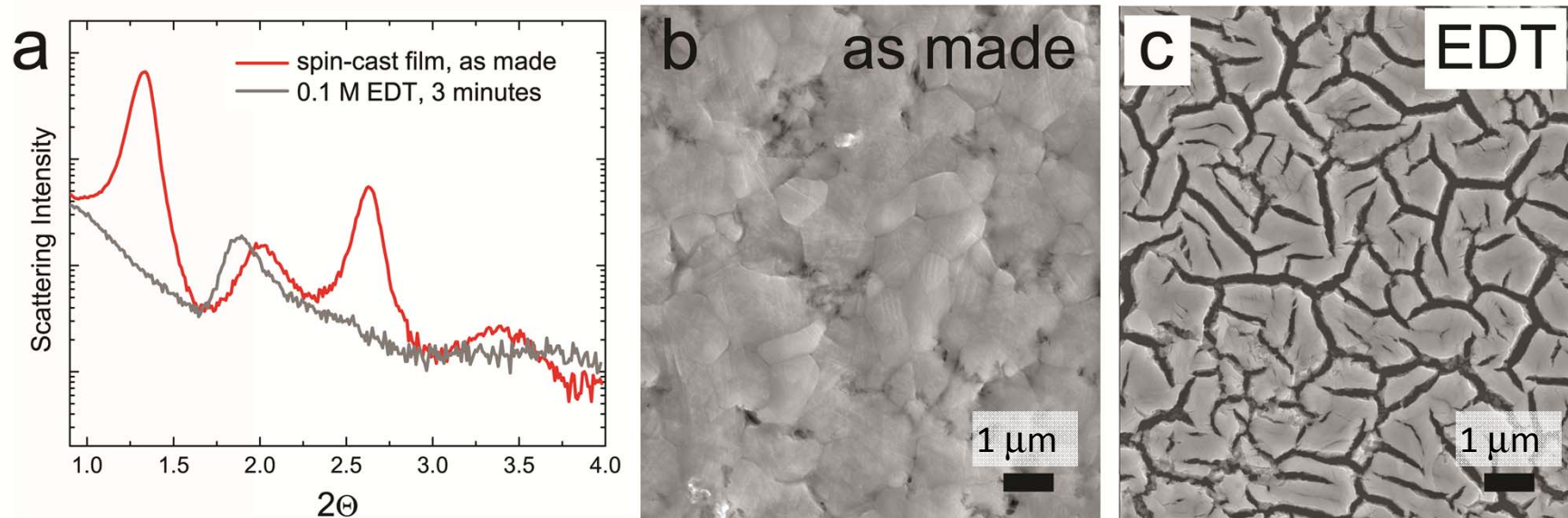
aniline (0.8 nm)

ethylenediamine (0.4 nm)

J. E. Murphy *et al.*, JACS **128**, 3241 (2006).



## Post-casting treatment of spin-cast films of PbSe NCs

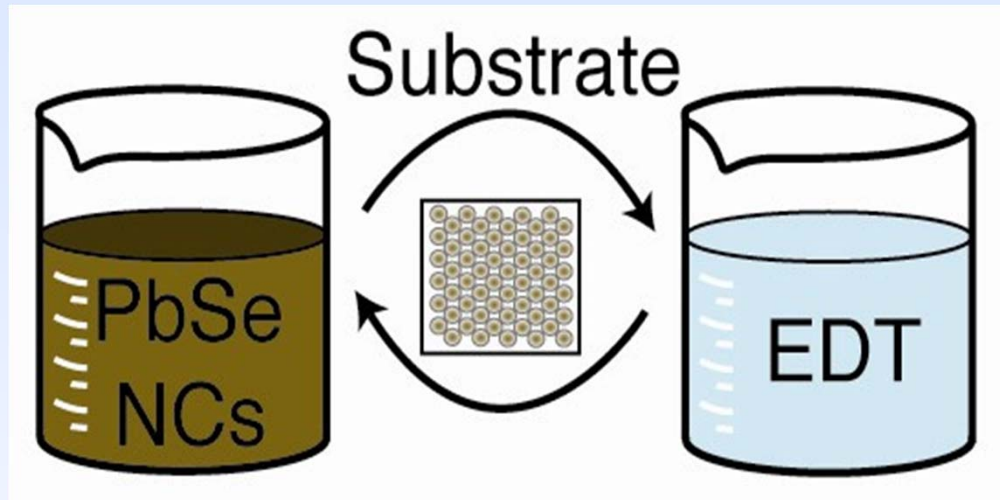


“Microstructure of the spin-cast NC films before and after EDT treatment. (a) SAXS data, showing a  $\sim 16 \text{ \AA}$  decrease in the spacing between the NCs and a dramatic loss of superlattice order upon EDT treatment. Measurements were taken in air. (b, c) Plan-view SEM images of (b) an untreated film and (c) a treated film.”

J. Luther, M. Law et al., ACS Nano 2, 271 (2008).



## Layer-by-layer fabrication of PbSe NC films



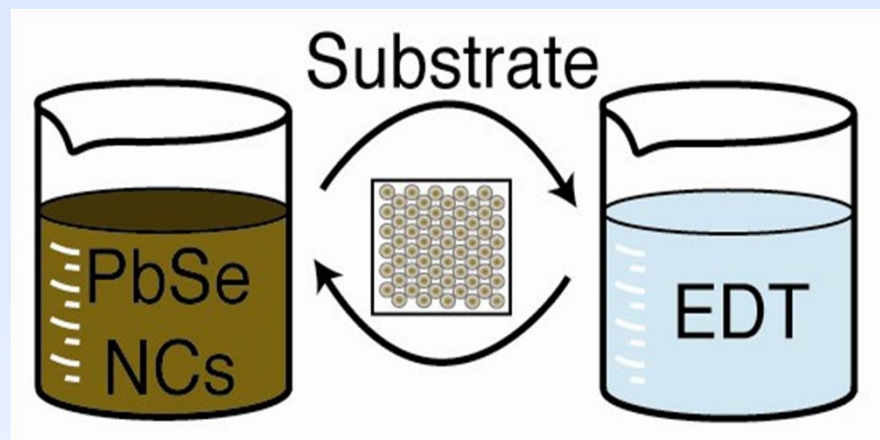
EDT = 1,2-ethanedithiol

**Layer by layer (LbL) fabrication of PbSe nanocrystal (NC) films.** Nanocrystal films prepared by dip-coating, alternating between (1) PbSe NCs in hexane and (2) 0.1 M EDT in anhydrous acetonitrile, allowing the film to dry between each layer.

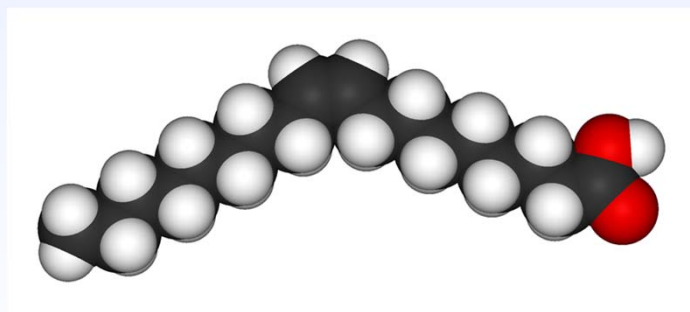
J. M. Luther, M. Law *et al.*, "Structural, Optical, and Electrical Properties of Self-Assembled Films of PbSe Nanocrystals Treated with 1,2-Ethanedithiol", *ACS Nano* **2**, 271 (2008).



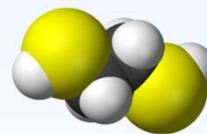
## Ligand exchange in PbX NC films



EDT = 1,2-ethanedithiol



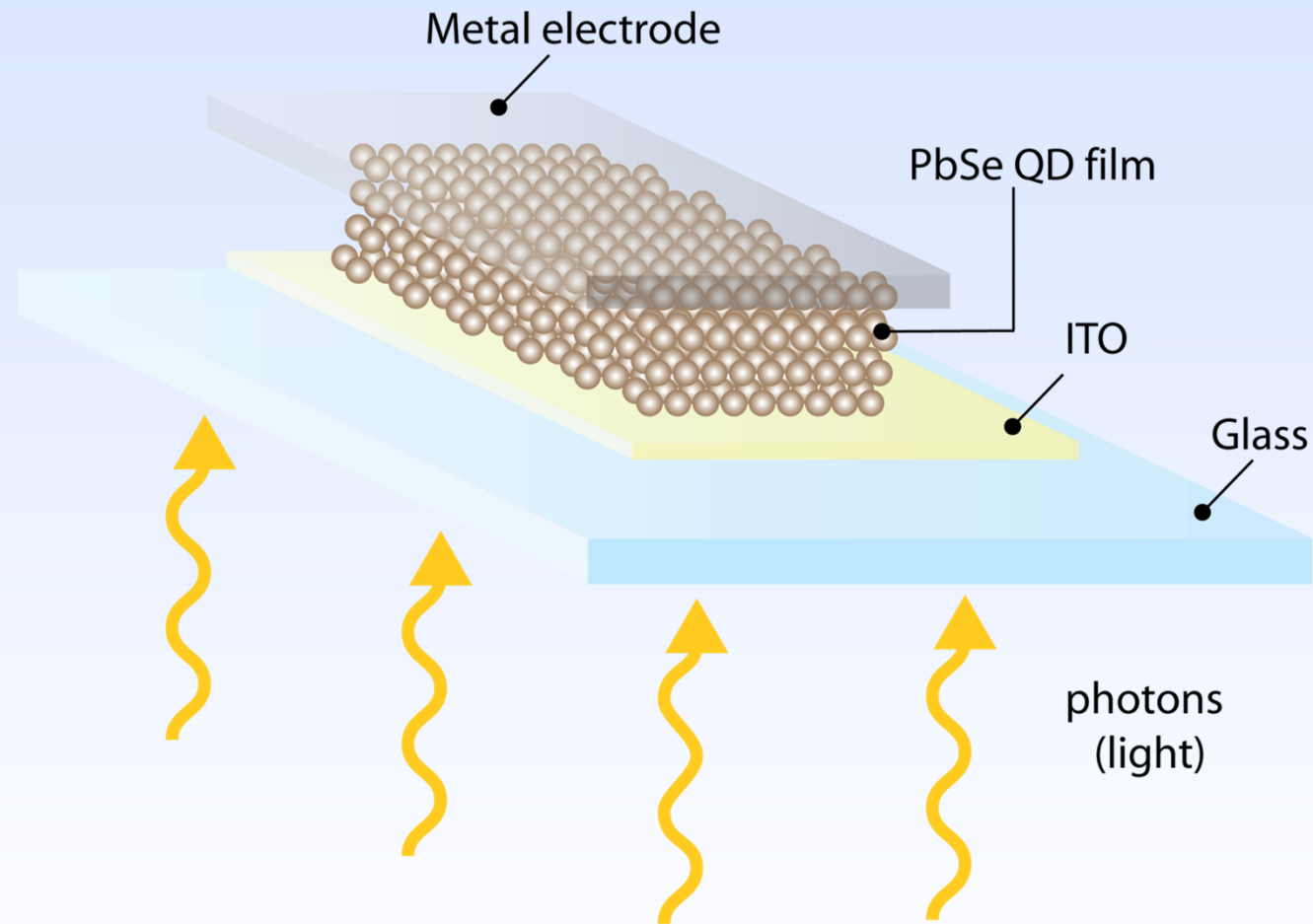
Oleic acid,  $C_{18}H_{34}O_2$   
 $L \approx 20 \text{ \AA}$



1,2-ethanedithiol  
 $C_2H_6S_2$   
 $L \approx 6 \text{ \AA}$



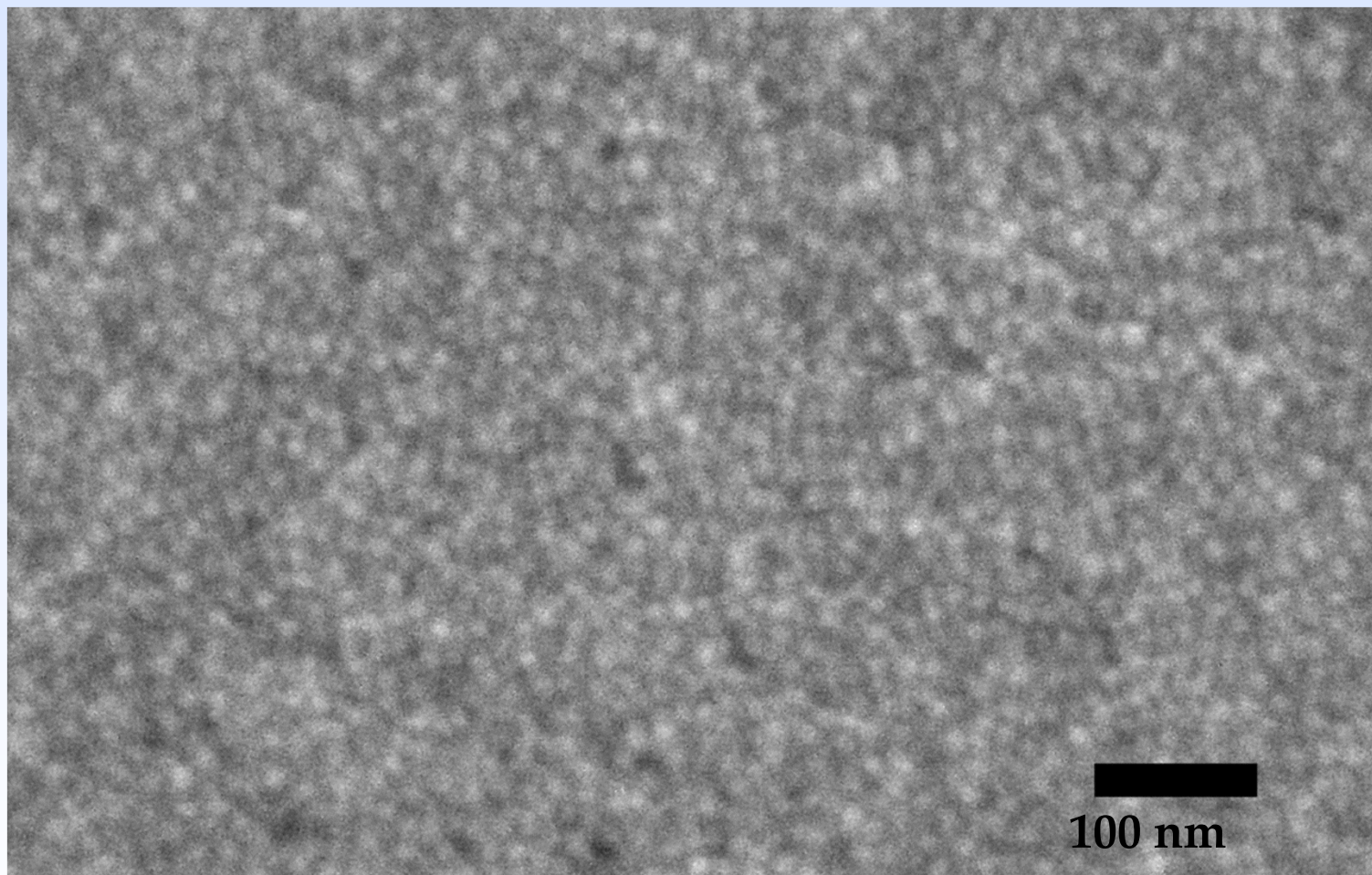
# Schottky barrier nanocrystal-based solar cell



- For MEG: Auger recombination typically occurs on  $\lesssim 100$  ps timescale (need fast exciton dissociation and/or diffusion to low density)
- High long-range mobility desired
- EQE > 100% would provide MEG process/concept confirmation



# Layer-by-layer dip-coated PbSe films

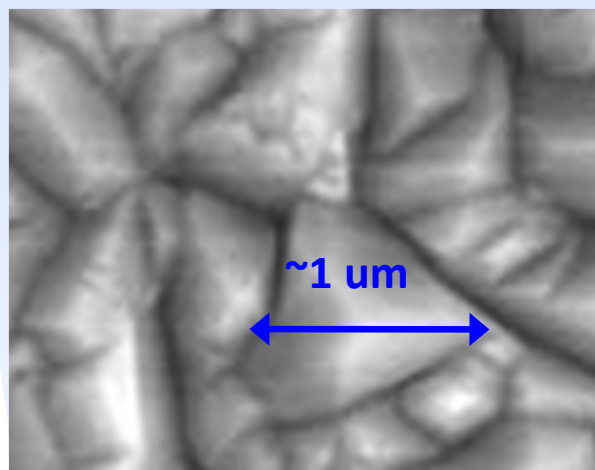


Plan view SEM image of PbSe NC films prepared by layer-by-layer dip coating onto ITO substrate. LbL film shown was produced using 10-20 dip coating cycles.

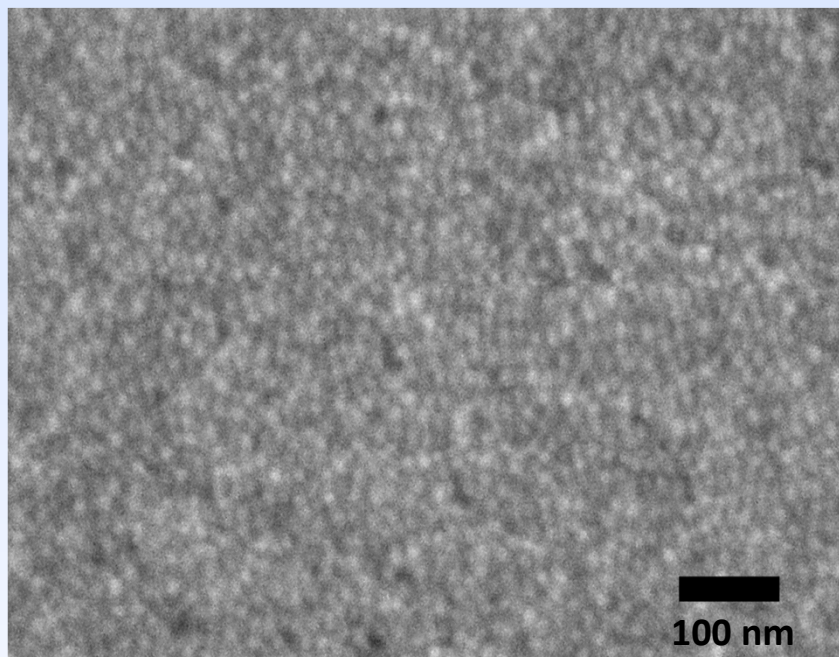
J. Luther, M. Law *et al.*, *ACS Nano* **2**, 271 (2008).



## “Grain boundary” density considerations



e.g. CdTe



Estimating effective “grain boundary densities” (boundary area / layer area)

**CdTe:**  $\sim 1 \mu\text{m}$  grain size (assumed cubic grains,  $\sim 1 \mu\text{m}$  thick layer):

**3 ( $\mu\text{m}^2 / \mu\text{m}^2$ )**

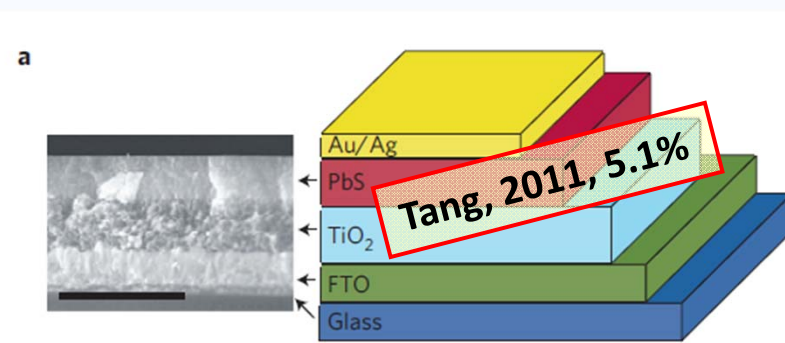
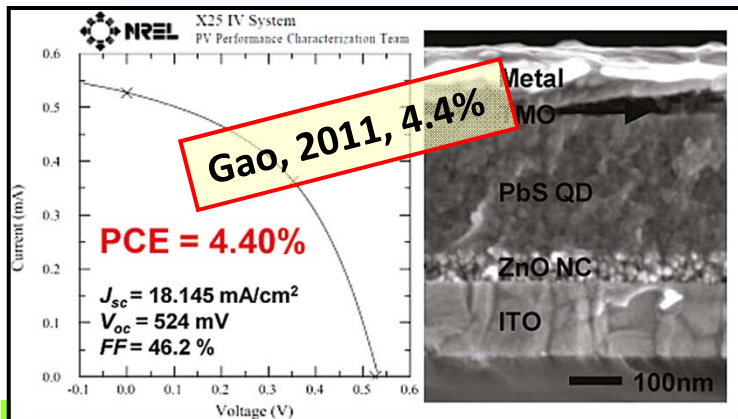
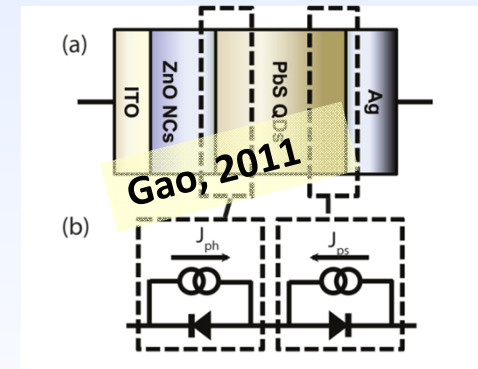
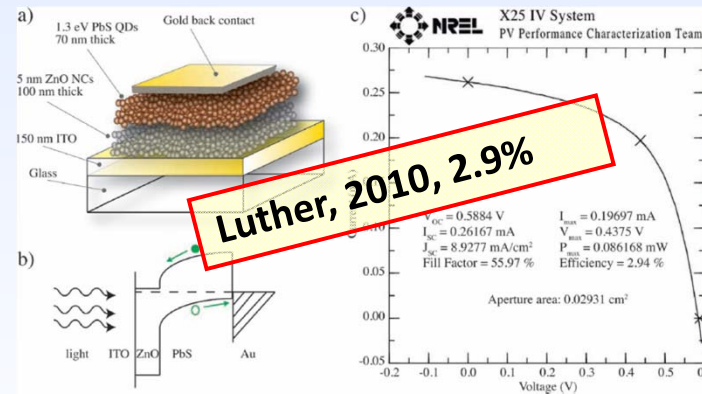
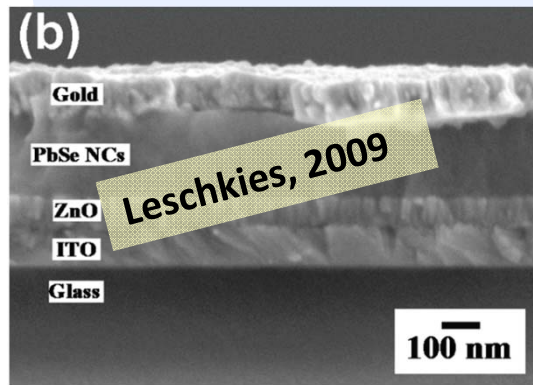
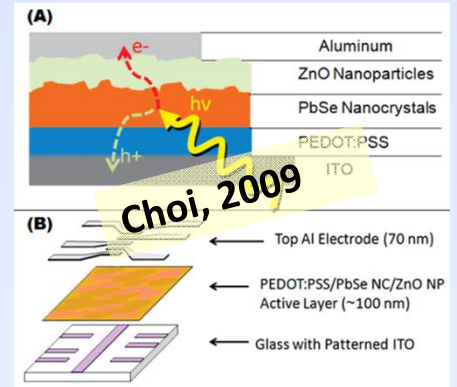
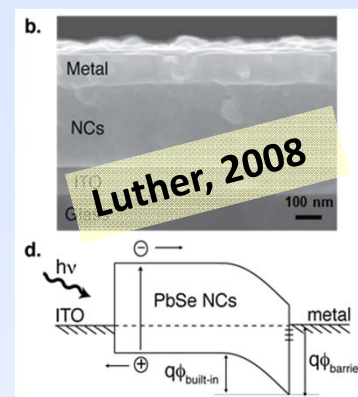
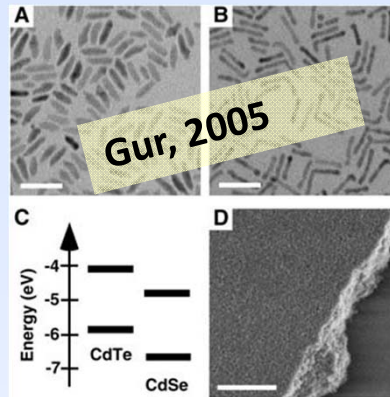
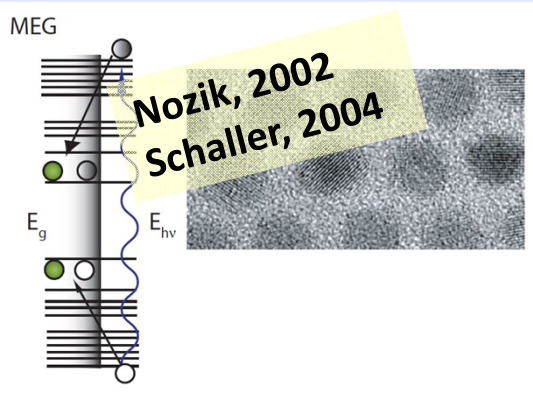
**PbSe QD film:**  $\sim 5 \text{ nm}$  “grain size” (assumed cubic grains 5 nm on a side,  $1 \mu\text{m}$  thick film):

**600 ( $\mu\text{m}^2 / \mu\text{m}^2$ )**

$$S/V \propto 1/r$$



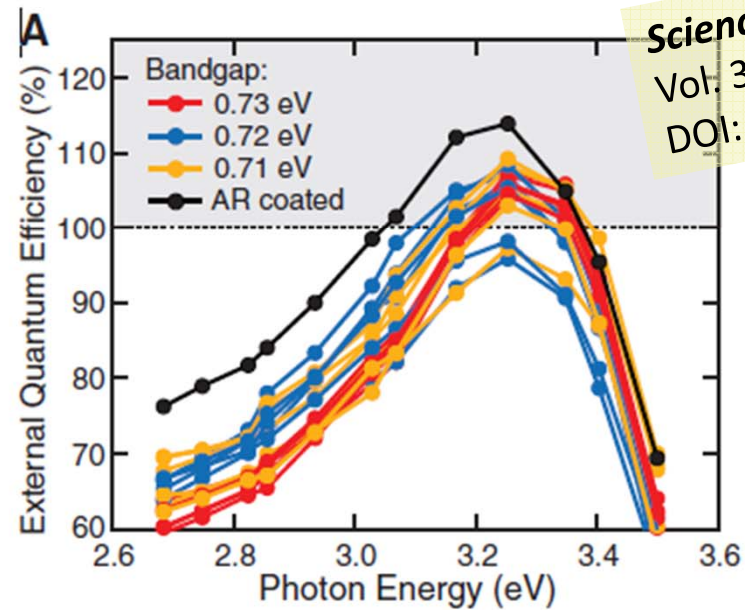
# Directions in QD-based solar cell research





# Peak External Photocurrent Quantum Efficiency Exceeding 100% via MEG in a Quantum Dot Solar Cell

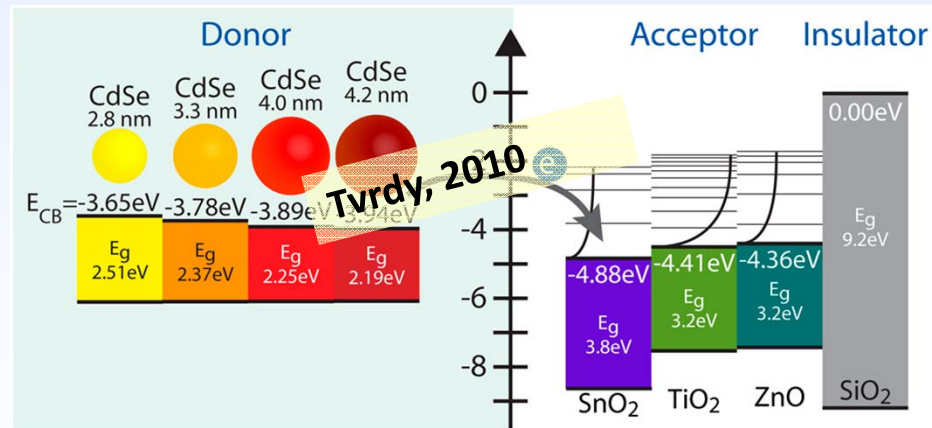
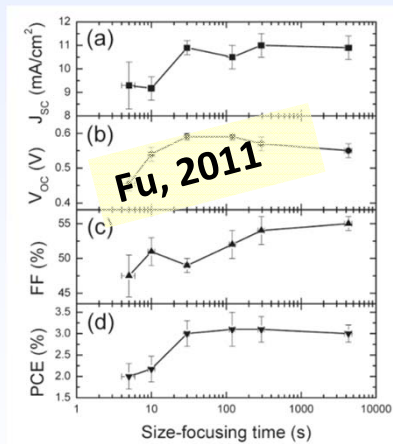
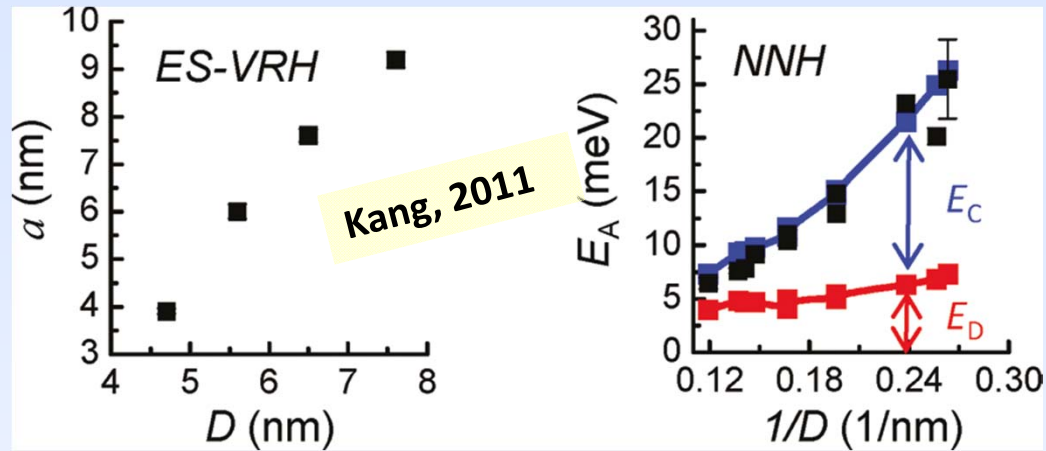
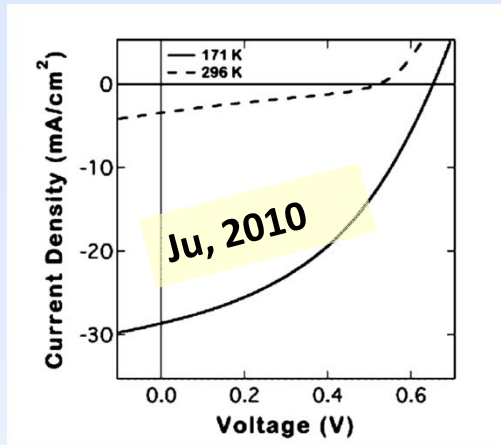
Octavi E. Semonin,<sup>1,2</sup> Joseph M. Luther,<sup>1</sup> Sukgeun Choi,<sup>1</sup> Hsiang-Yu Chen,<sup>1</sup> Jianbo Gao,<sup>1,3</sup> Arthur J. Nozik,<sup>1,4\*</sup> Matthew C. Beard<sup>1\*</sup>



*Science* 16 December 2011:  
Vol. 334 no. 6062 pp. 1530-1533  
DOI: 10.1126/science.1209845



# Directions in QD-based solar cell research



**Many others  
2002-2012**



## Roll-to-roll processing from solution source (e.g., Nanosolar CIGS)

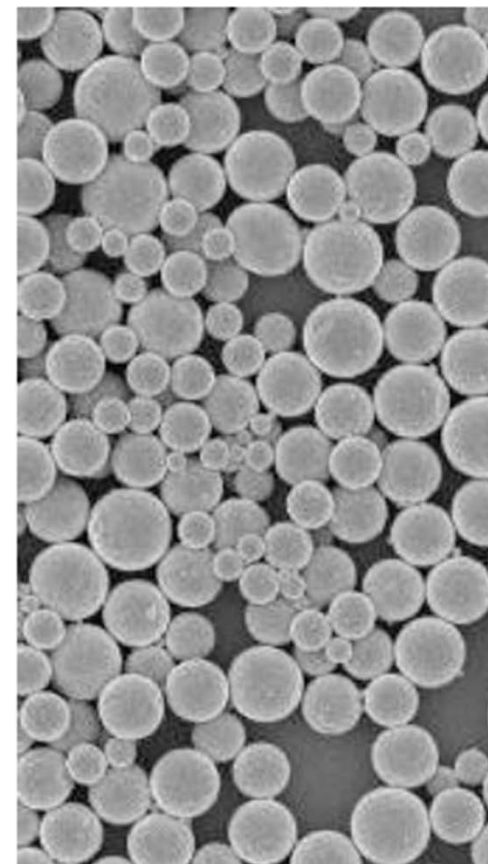


**Figure 6 and 7:** A laboratory sample of our nanoparticle ink. Nanoparticles shown to the right are an average of 20nm in diameter.

from NanoSolar white paper

.... energizing Ohio for the 21st Century



# Good solar cells from nanoparticle inks (CIGS)

## Nanosolar CdS/Cu(In,Ga)Se<sub>2</sub> Cell

Device ID: H09B071-01C #2

Device Temperature: 24.0

Apr 09, 2009 12:31

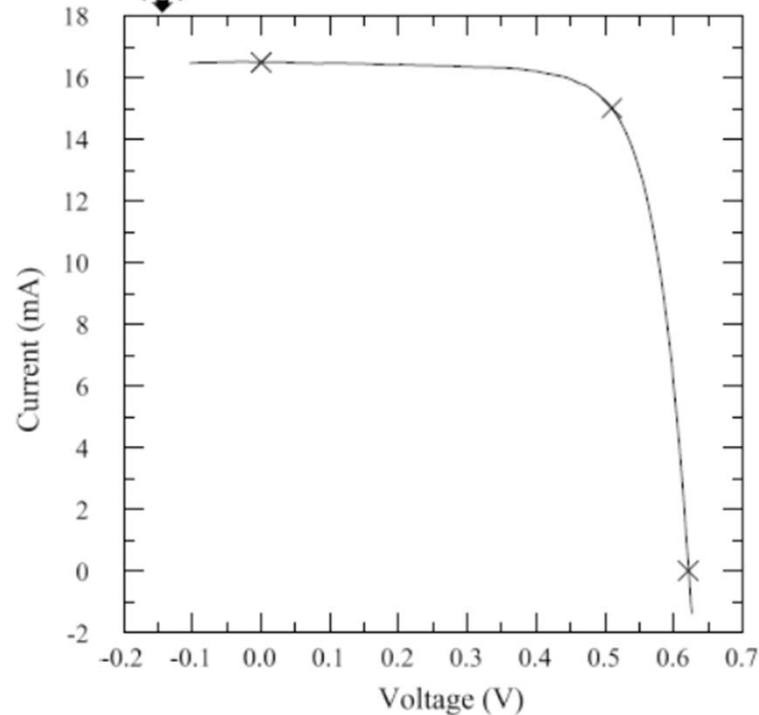
Device Area: 0.5000 cm<sup>2</sup>

Spectrum: ASTM G173 global

Irradiance: 1000.0 W/m<sup>2</sup>



X25 IV System Confidential  
PV Performance Characterization Team



$V_{oc} = 0.6214$  V  
 $I_{sc} = 16.490$  mA  
 $J_{sc} = 32.980$  mA/cm<sup>2</sup>  
Fill Factor = 74.70 %

$I_{max} = 15.010$  mA  
 $V_{max} = 0.5101$  V  
 $P_{max} = 7.6540$  mW  
Efficiency = 15.31 %

from NanoSolar white paper

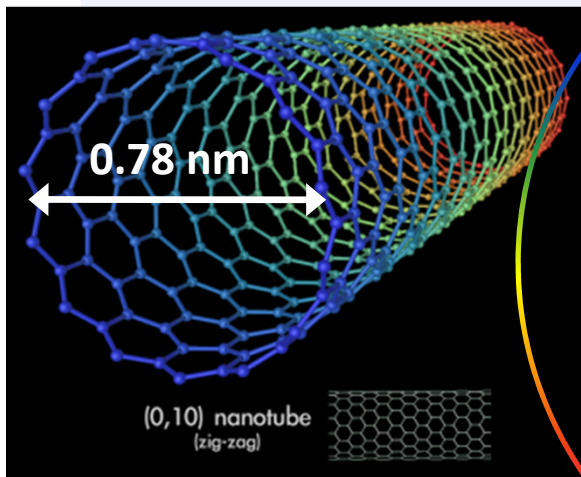


# Colloidal semiconductor nanocrystals

- Solution synthesis, typically at elevated temperature
- Inorganic crystalline core surrounded by organic capping molecules
- Most frequently suspended in organic solvents
- Can be stored stably either in powder or solution form

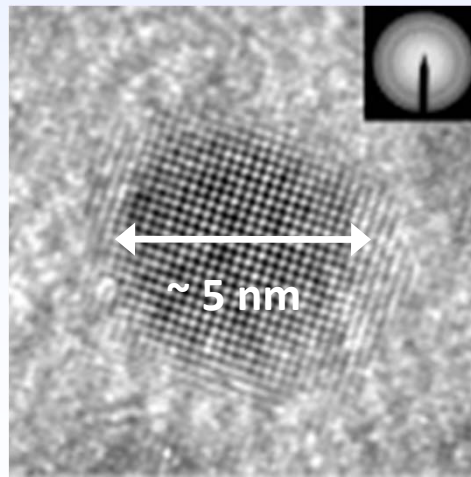
Colloidal semiconductor NCs have typical diameters of 1 nm to 10 nm

SWNT (10,0)



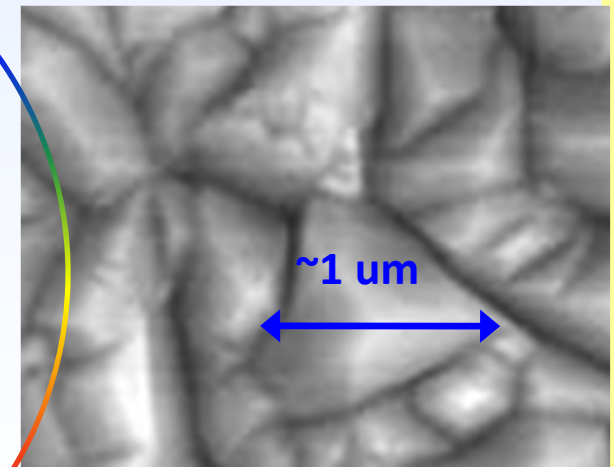
[http://commons.wikimedia.org/wiki/Main\\_Page](http://commons.wikimedia.org/wiki/Main_Page)

PbS NC



Sargent, *Adv. Mat.* (2005), 515-522.

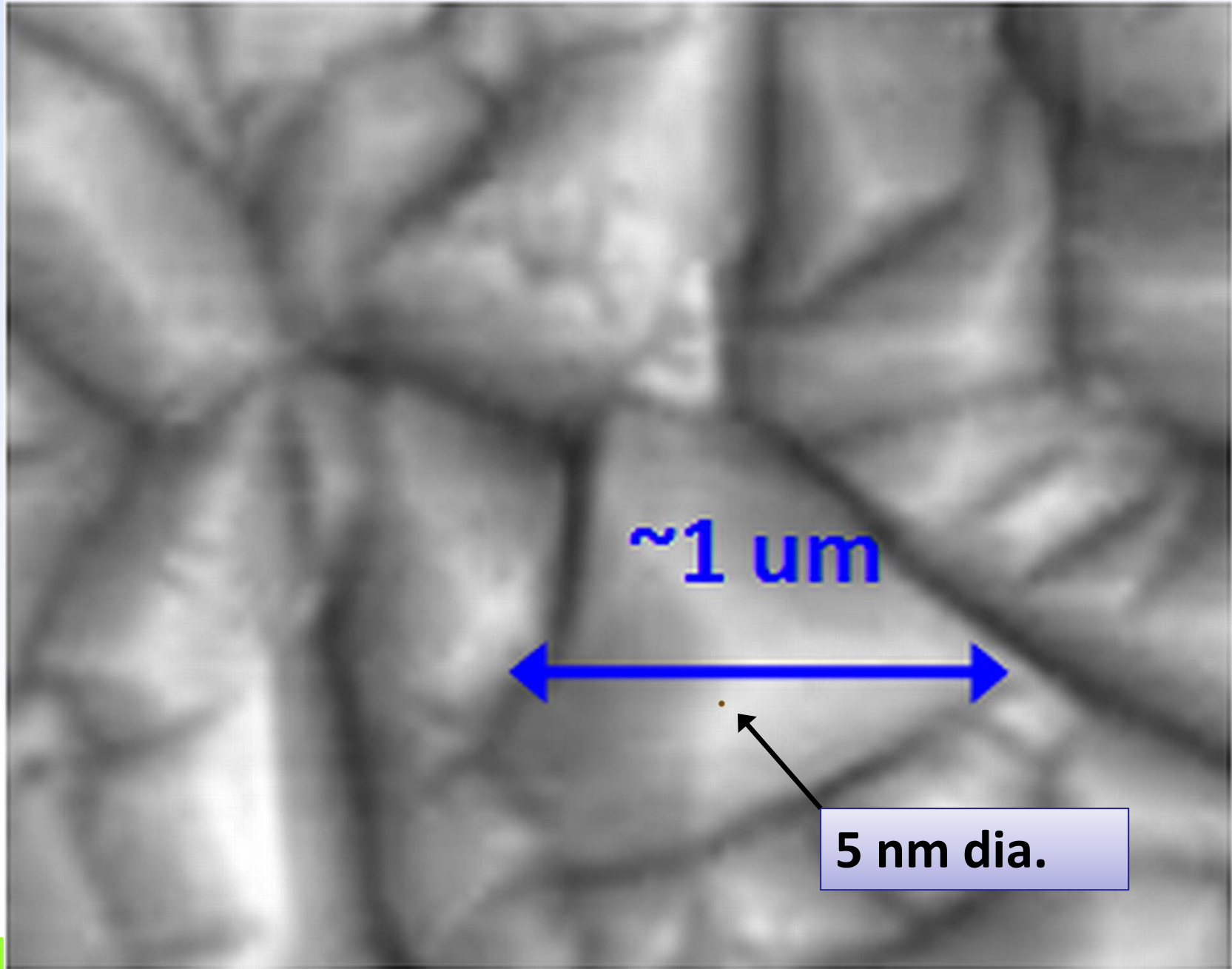
CdTe grain size (CSS)



Quiñones et al., *J. Mater. Sci: Mat. Electron* (2007), 1085–1091



# Colloidal quantum dot – scale



# Coupling QDs within a film (or array)

9794 *J. Phys. Chem. B*, Vol. 102, No. 49, 1998

Micic et al.

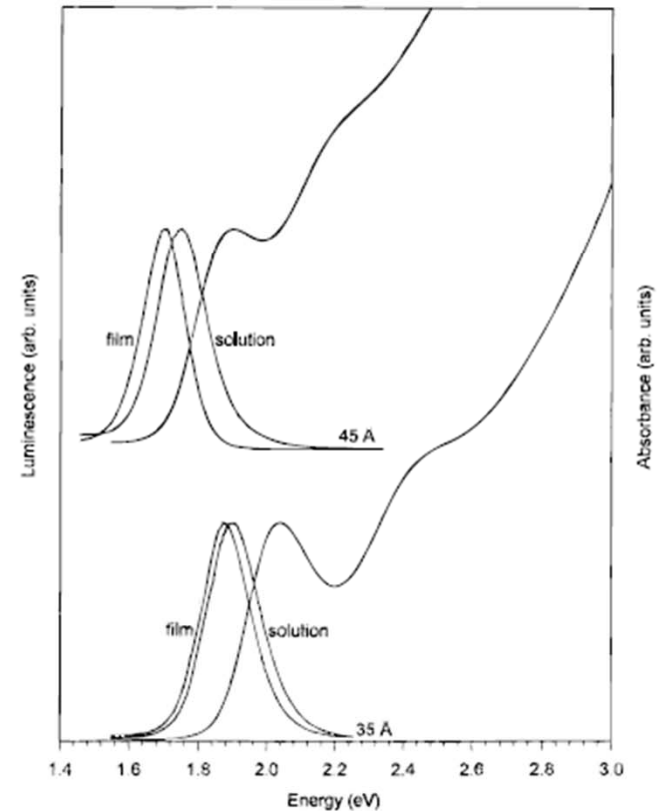
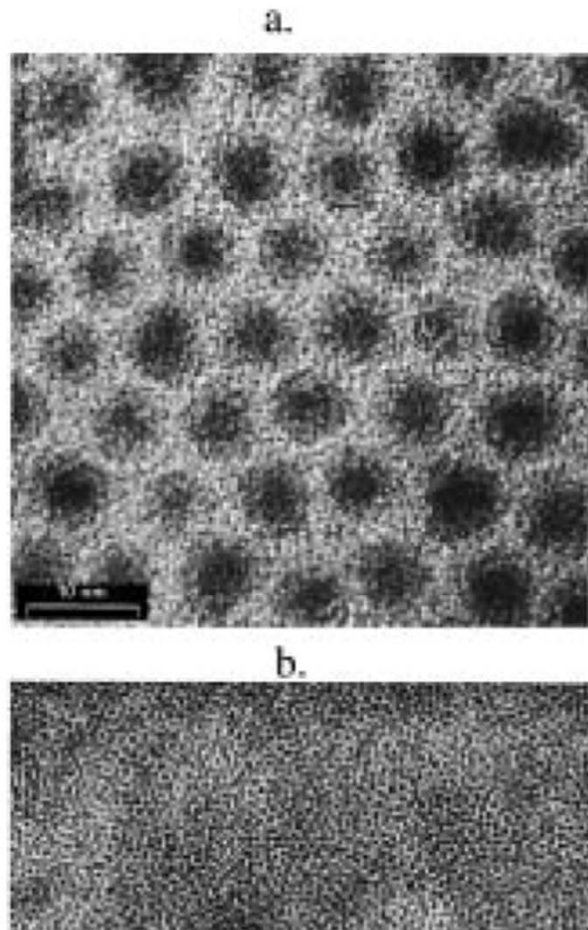


Figure 6. Absorption and luminescence spectra ( $\lambda_{\text{exc}} = 500 \text{ nm}$ ) of InP QDs in dilute colloidal solution and in close-packed films for 45- and 35-Å diameter QDs.



# Coupling mechanisms

What could cause a decrease in QD-QD spacing to red-shift the exciton transition?

“This can cause (i) an increase in the average dielectric constant of the film, (ii) an increase in the inter-QD radiative coupling, and (iii) an increase in the inter-QD electronic coupling.”

*Strong Electronic Coupling in Two-Dimensional Assemblies of Colloidal PbSe Quantum Dots*, Williams et al., ACS Nano (2009)

- i) Increased wavefunction extension
- ii) Increased FRET
- iii) Reduced barrier width for tunneling/hopping transport

$$a_B^* = \left( \frac{\epsilon m_e}{\epsilon_0 m_r^*} \right) 0.053 \text{ nm}$$



Kopf, R. F., E. F. Schubert, et al. (1993). "Modification of GaAs/AlGaAs growth-interrupted interfaces through changes in ambient conditions during growth." *Journal of Applied Physics* 74(10): 6139-6145.





# Energy/charge transport mechanisms

Energy transfer (FRET):

$$E = \frac{1}{1 + \left(\frac{r}{R_0}\right)^6}$$

$\Rightarrow R_0 \approx 8-9$  nm for  
 $\sim 3$  nm InP QDs

*J. Phys. Chem. B* **1998**, **102**, 9791-9796

Hopping/tunneling transport:

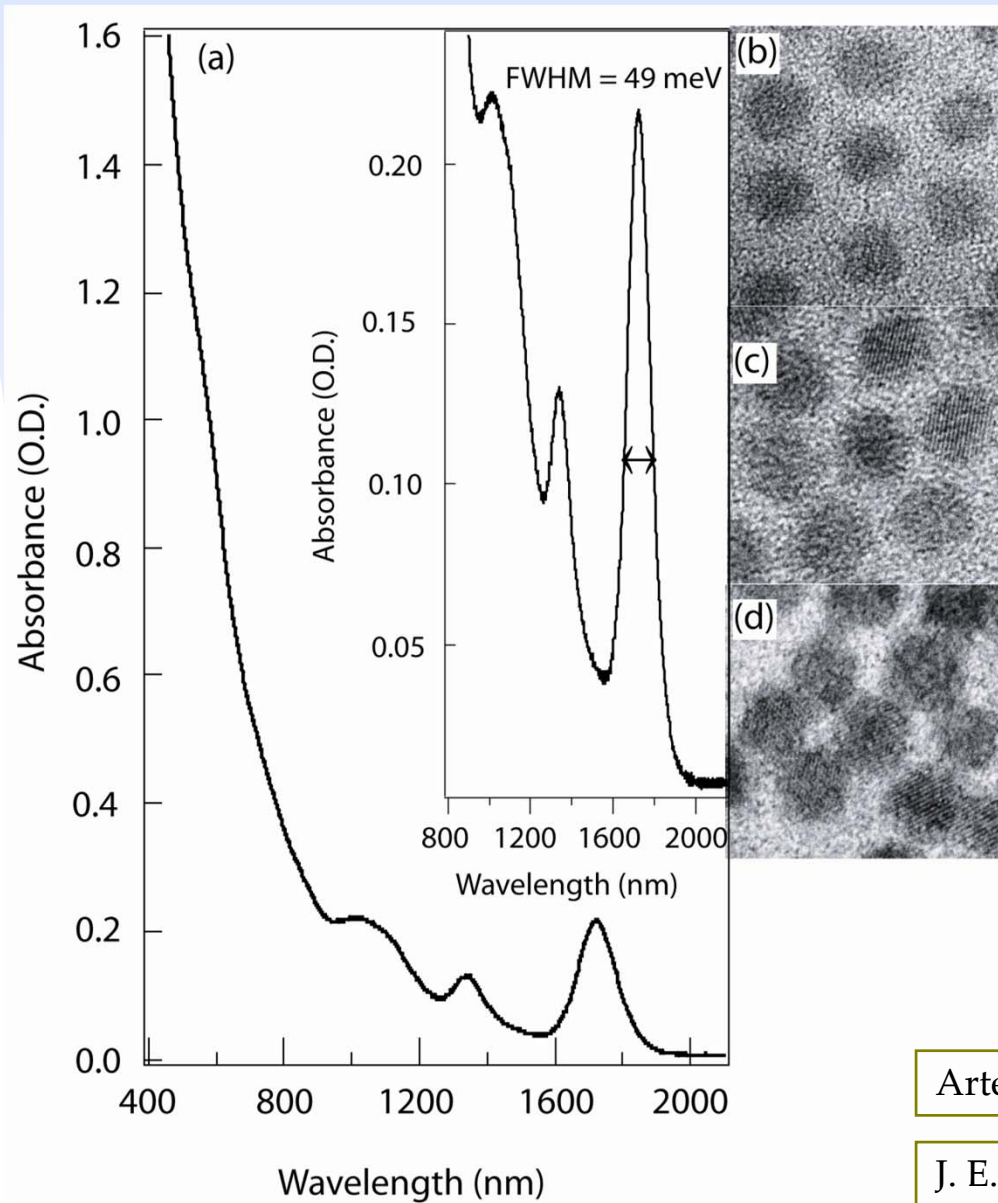
$$\Gamma_{ij} = \Gamma_0 \exp(-\beta d) \begin{cases} \exp\left[-\frac{E_j - E_i}{kT}\right] & E_j > E_i \\ 1 & E_i > E_j \end{cases}$$

Miller, Abrahams, *Phys. Rev.* **120**, 745–755 (1960)

Liu, Hillhouse, Law, *Nano Lett.* (2010), **10**, 1960.



## Post-deposition treatment of drop-cast films of 5.7 nm dia. PbSe QDs



oleic acid (1.8 nm)

aniline (0.8 nm)

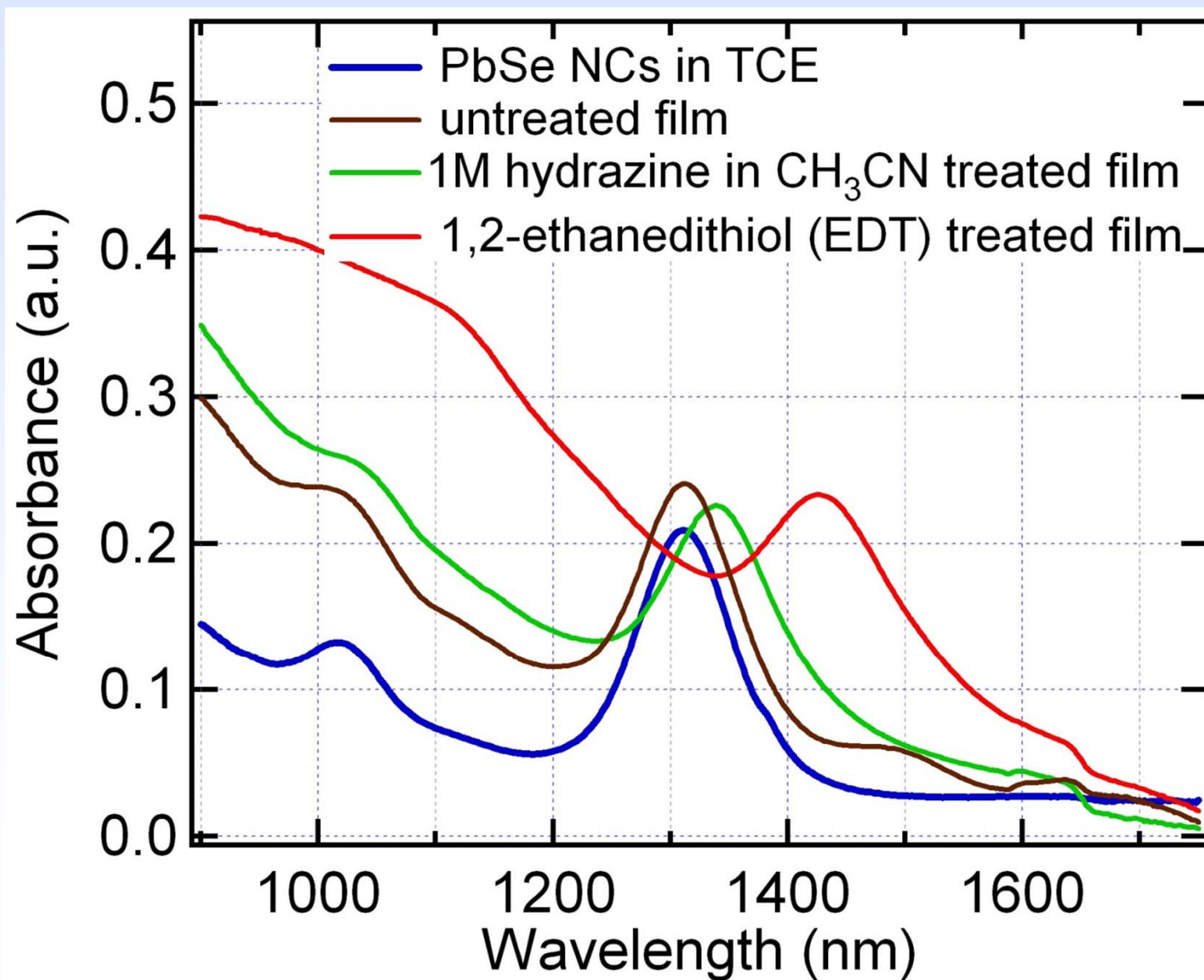
ethylenediamine (0.4 nm)

Artemyev *et al.*, J. Phys. Chem. B 2000, 11617.

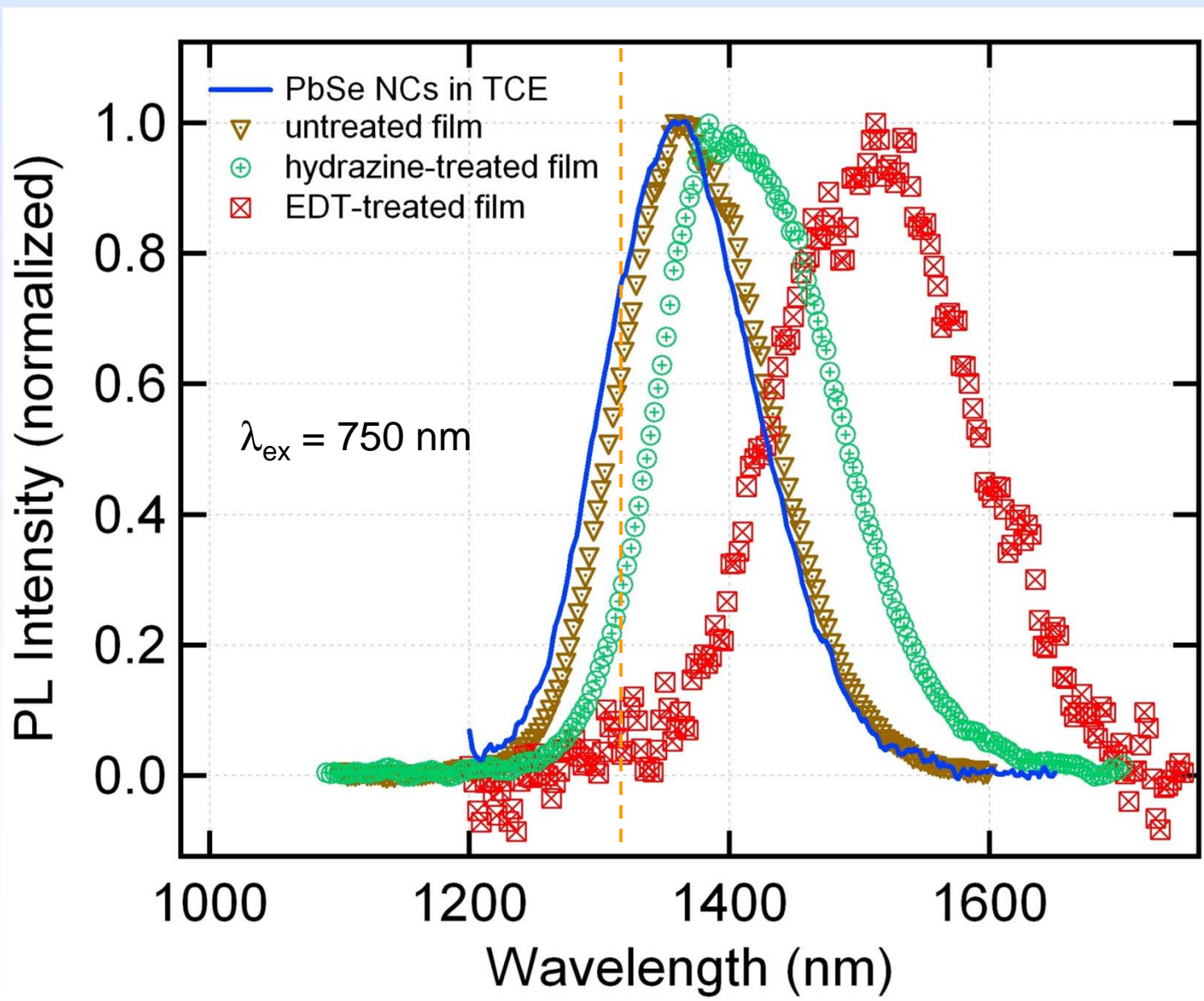
J. E. Murphy *et al.*, J. Phys. Chem. B 2006, 25455.



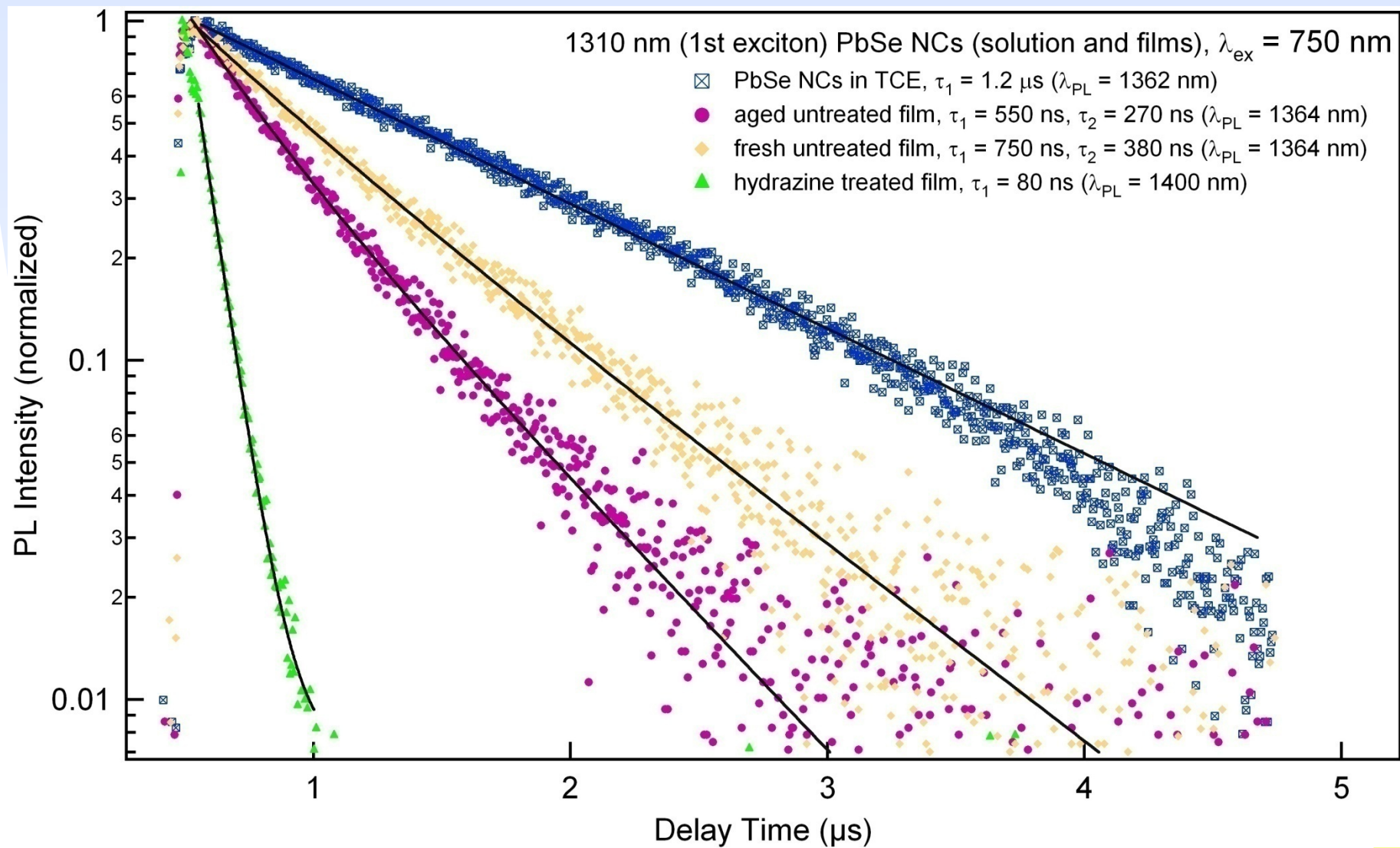
## Absorption spectra: spincast films of 1310 nm PbSe NCs



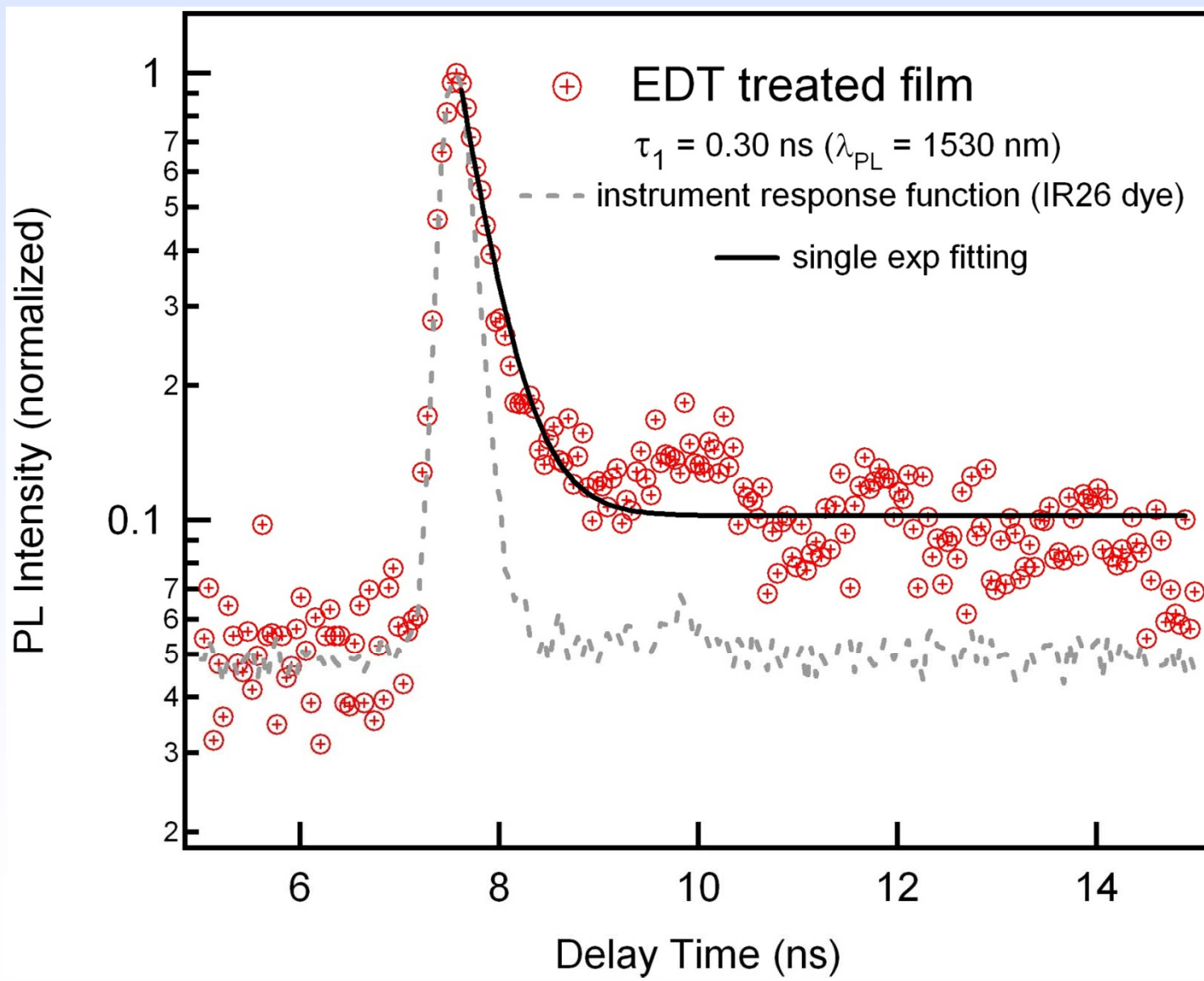
## Steady-state photoluminescence (1310 nm NCs)



# Time-resolved photoluminescence spectra

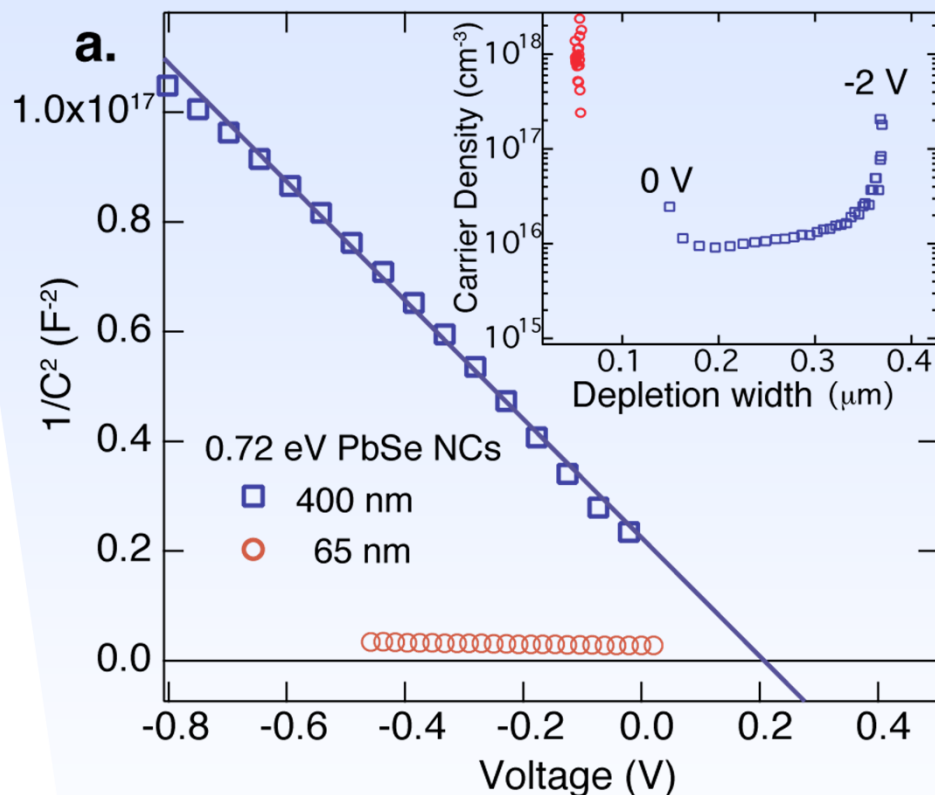


## PL lifetime for EDT-treated PbSe NC film



# Depletion width and doping density

J. M. Luther, M. Law, *et al.*, *Nano Lett.* **8**, 3488-3492 (2008).



“Mott-Schottky plots at 1 kHz for devices with a thin (65 nm, red) and thick (400 nm, blue) NC layer. The thick device has an equilibrium depletion width of ~150 nm, while the thin device is fully depleted.”

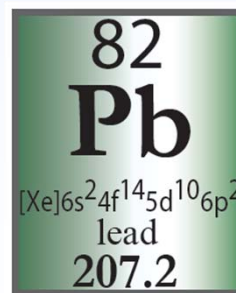
Relation between doping density and QD density? QD size ~ 6 nm dia., add 1 ligand ~0.5 nm, so  $V(\text{QD}) = (4\pi/3)(3.2 \text{ nm})^3 = 1.3 \times 10^{-19} \text{ cm}^3$

Random packing of spheres → ~ 0.64

→ Vol. density of QDs ~  $5 \times 10^{18} \text{ cm}^{-3}$

→ ~1 free carrier per 500 QDs

How/why?



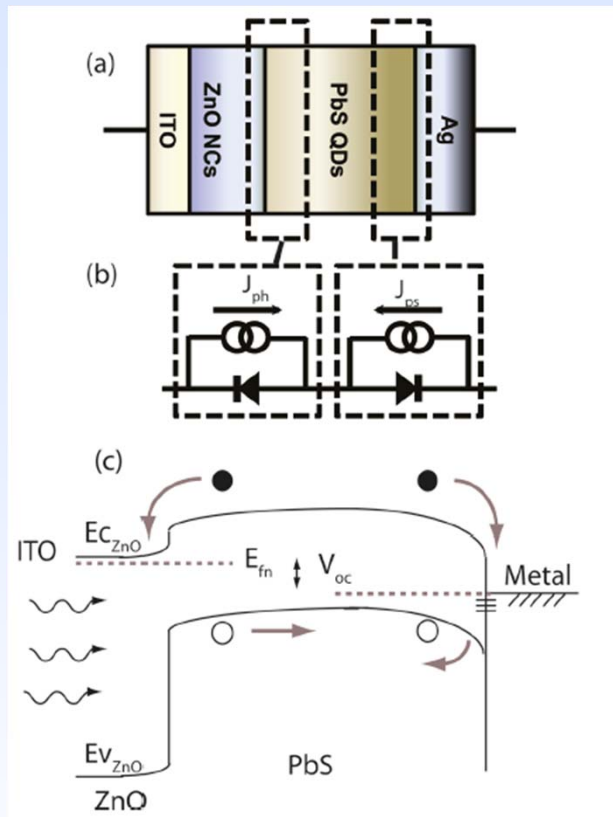
Pb-rich →  
n-type



S-rich →  
p-type



# Two-diode model for PbS/ZnO heterojunction device



Two-diode model equivalent circuit including a main diode between ZnO QD film with PbS QD film, and a Schottky-diode between PbS QD film with top contact Au or Ag.

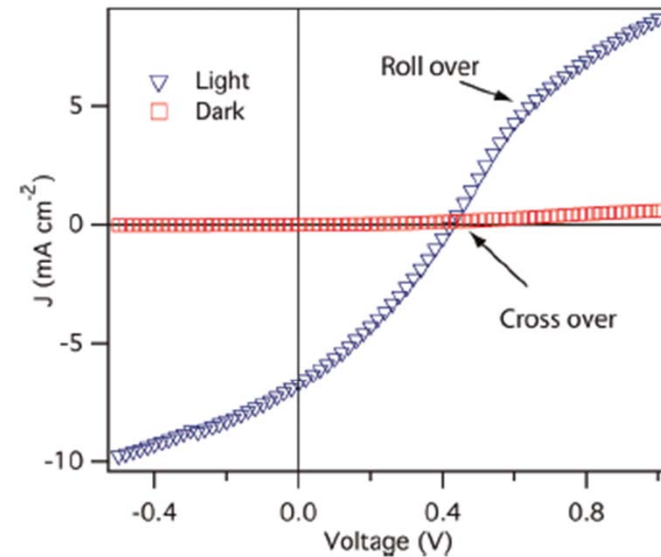


**Figure 1.** Typical characteristics of  $J-V$  in the dark and under 1 sun illumination, which shows the crossover and roll-over effects. The device structure is ITO/ZnO NC/PbS QD/Ag with PbS layer thickness of  $\sim 550$  nm.

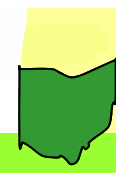
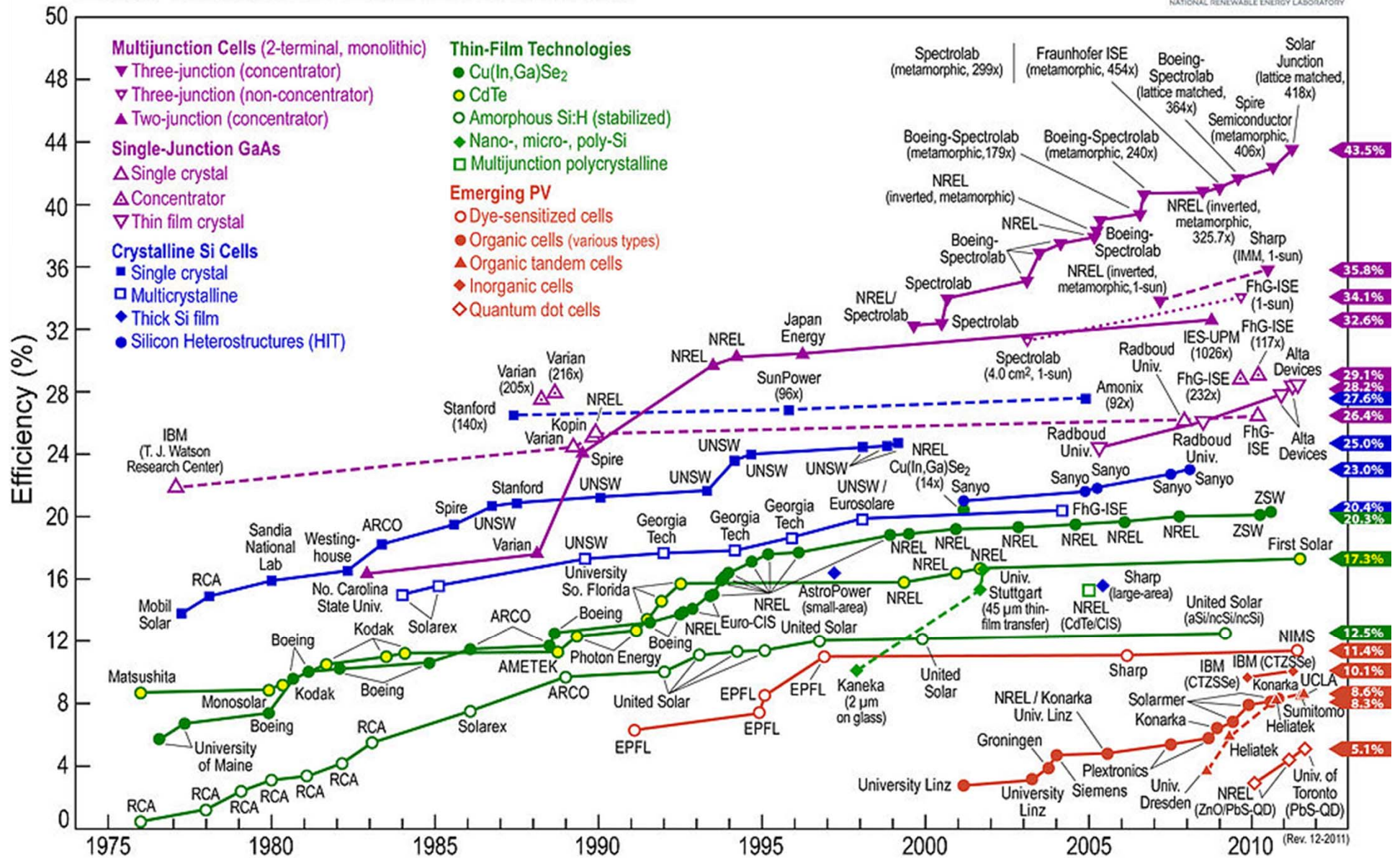
1. **Roll-over effect**, a fact of current limiting at positive voltage, is due to a hole transport barrier at Schottky-junction formed by PbS QD film with metal contact .
2. **Cross-over effect**: low forward current due to Schottky barrier at metal contact (hole transfer barrier).

“Quantum Dot Size Dependent  $J-V$  Characteristics in Heterojunction ZnO/PbS Quantum Dot Solar Cells”, J. Gao et al, Nano Lett. 2011.





# Best Research-Cell Efficiencies

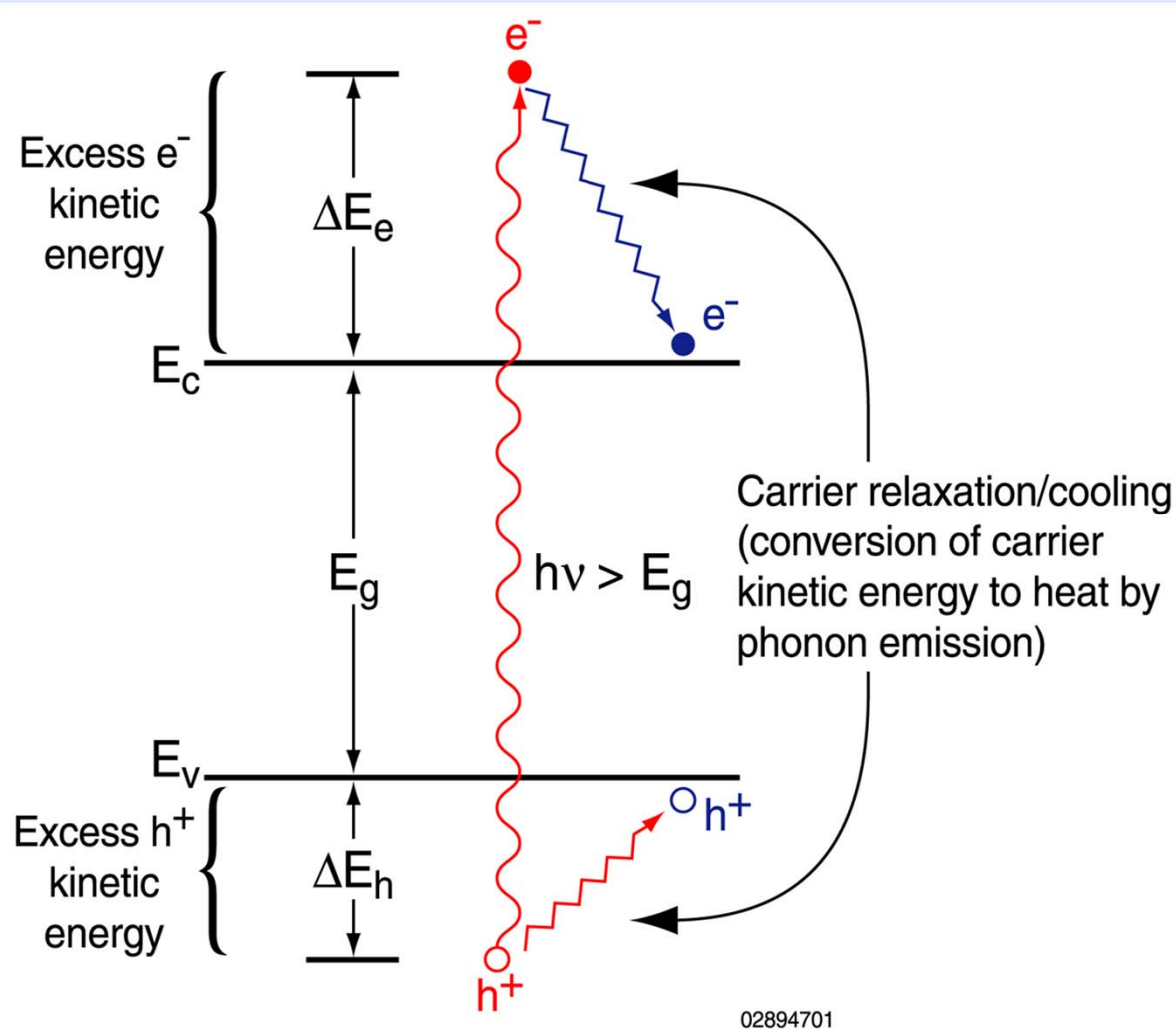


## Issues of interest for QD-based thin film PV

- Energy intensity of materials and deposition
- Doping control within films
- Air/moisture tolerance (deposition and operation)



# Thermalization losses



For  $c$ -Si ( $E_g = 1.1$  eV)  
at  $T = 300$  K, AM1.5G

$$\eta_{max} = 32.9\%$$

Losses

transmission = 18.7%

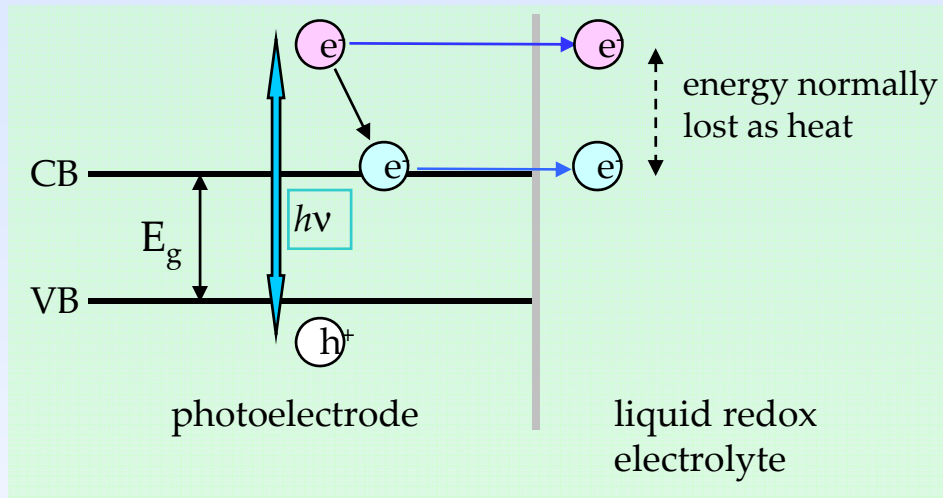
radiative em. = 1.6%

**heat** = 46.8%



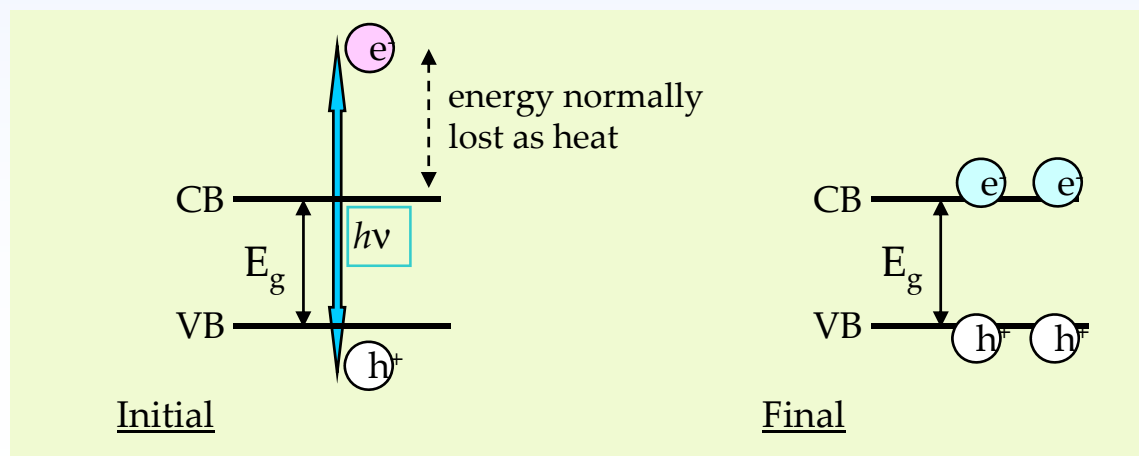
# Utilize photogenerated hot electrons to increase efficiency

1. **Higher photovoltage:** extract and utilize hot electrons



1 photon  $\rightarrow$   
1 hot electron

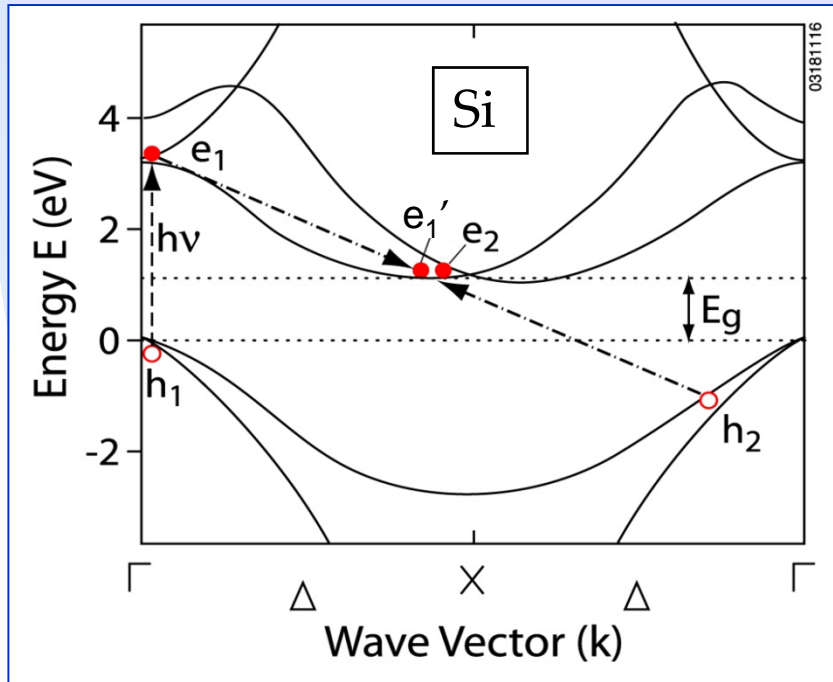
2. **Higher photocurrent:** carrier multiplication through impact ionization (inverse Auger process)



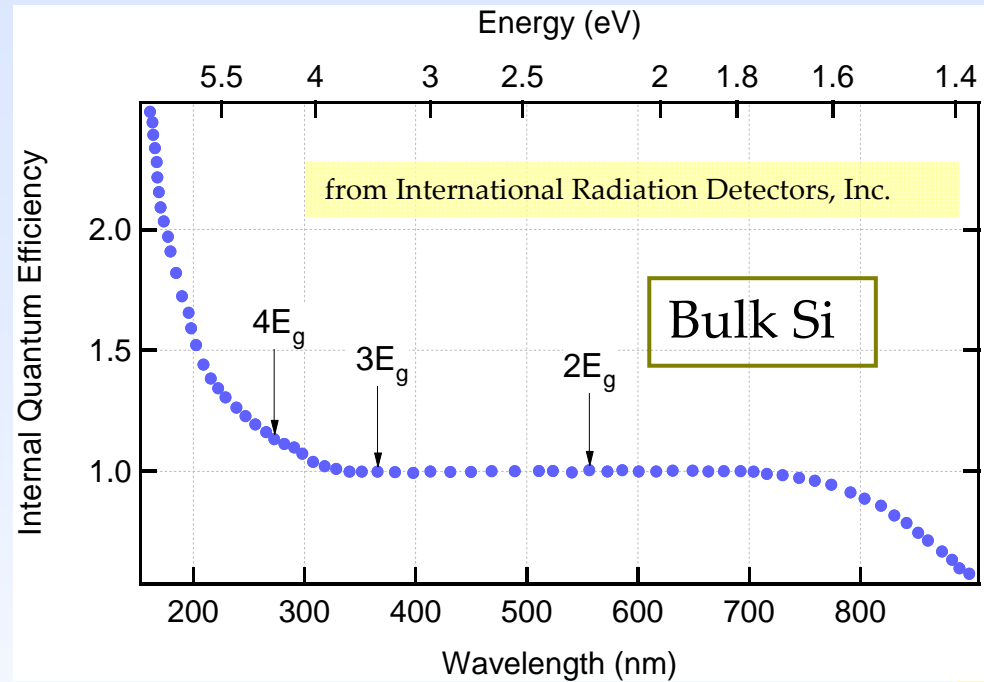
1 photon  $\rightarrow$   
2 (or more)  
cooled  
electrons



# Impact ionization in bulk semiconductors



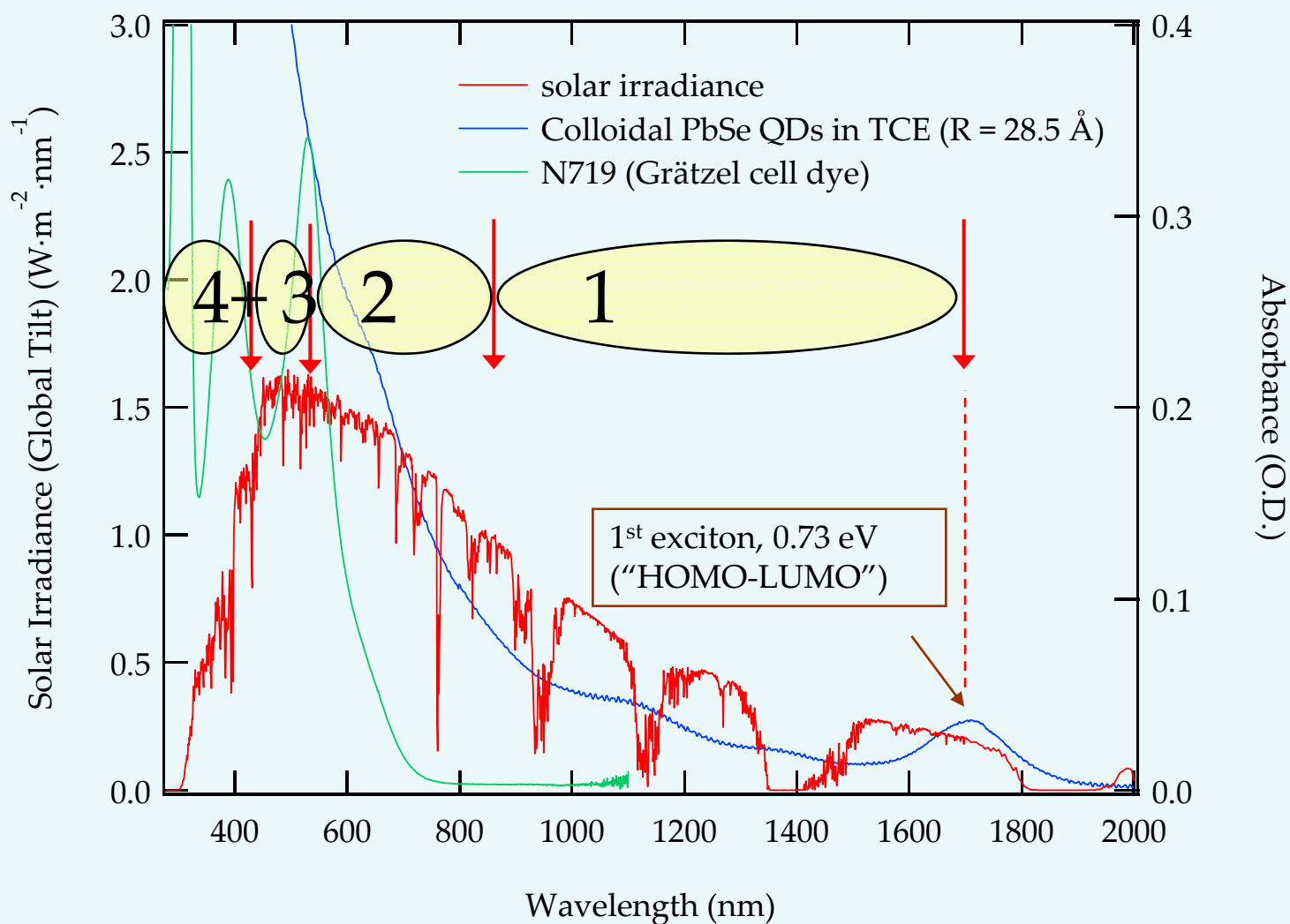
From Quiesser *et al.*, Appl. Phys. Lett. (1993).



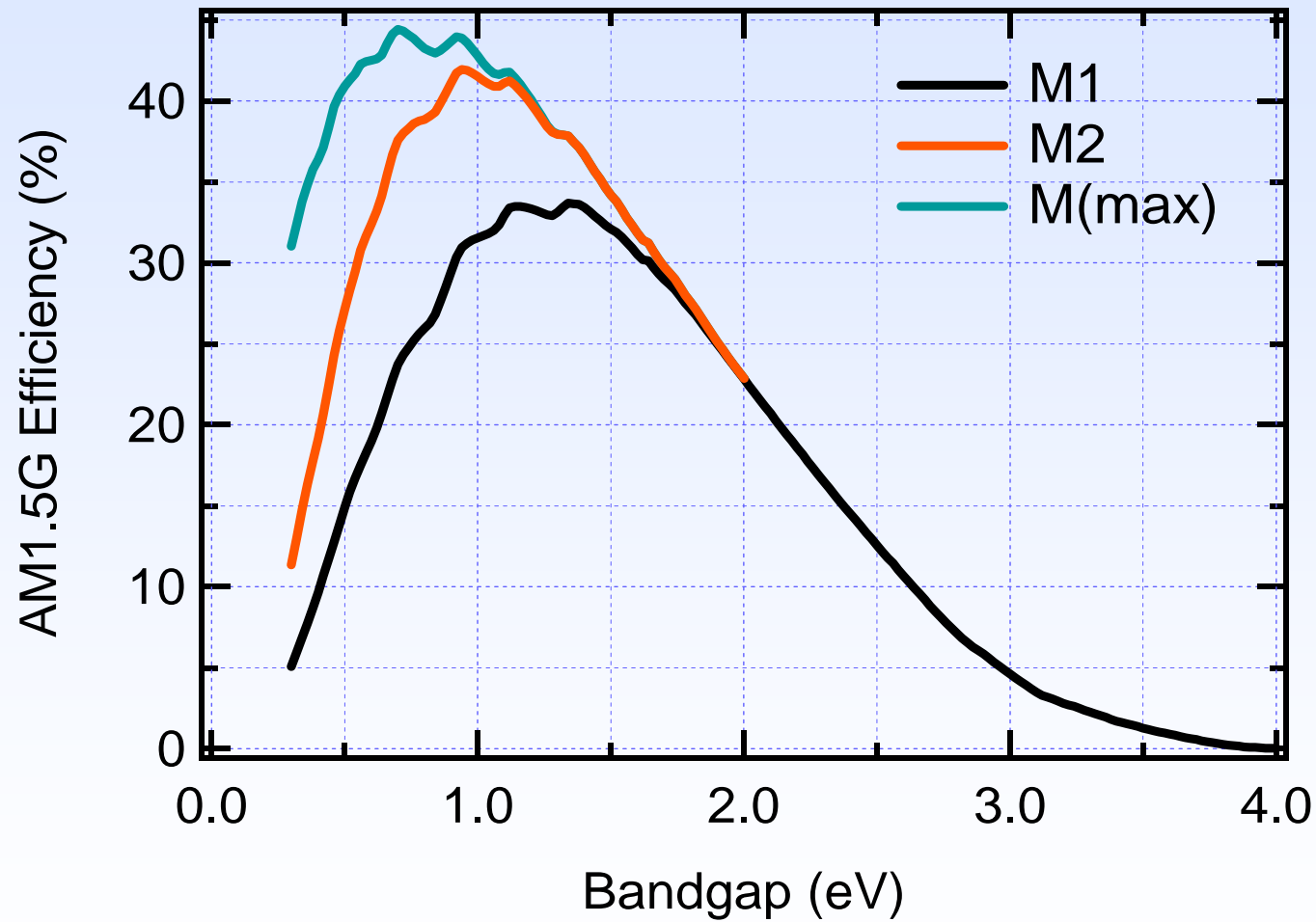
- Bulk Silicon ( $E_g \approx 1.1$  eV) exhibits an I.I. QY of just 1.2  $e^-h^+$  pairs per photon absorbed at 4.5 eV ( $\lambda = 275$  nm,  $hc/\lambda > 4 E_g$ ).
- Electron-phonon scattering dominates over I. I. up to very high photon energies.
- Nanocrystals exhibit a *reduced* momentum conservation requirement (NC surface can supply or absorb momentum during scattering processes).

# Enhancing conversion efficiency using NCs & MEG

## Matching absorption to solar irradiance spectrum



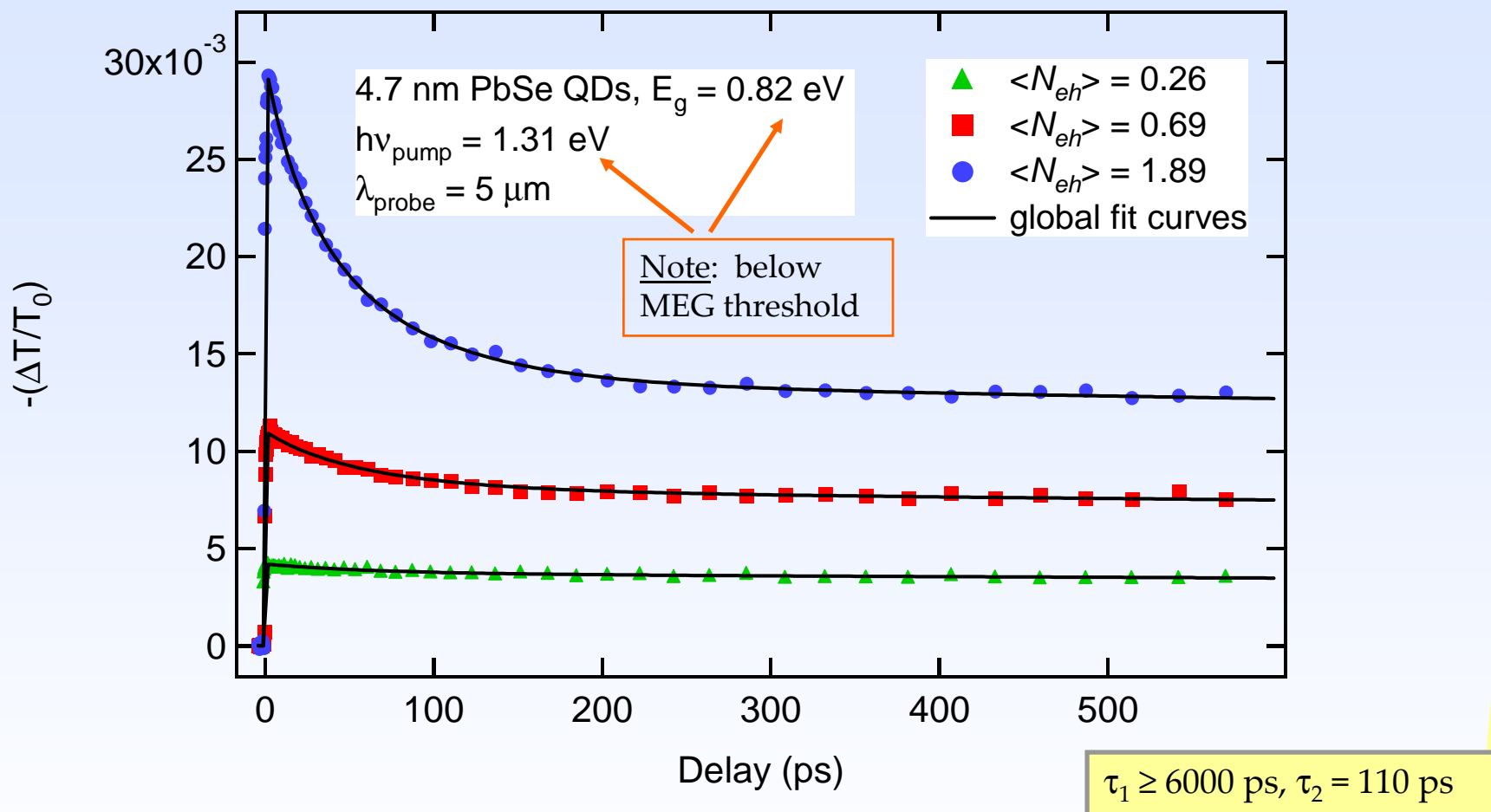
# MEG-active solar cells – efficiency limitations



*from Mark Hanna, NREL*



# Signature of multiple excitons: Auger recombination



Global fit for three intensities; excitation *below* the MEG threshold energy:

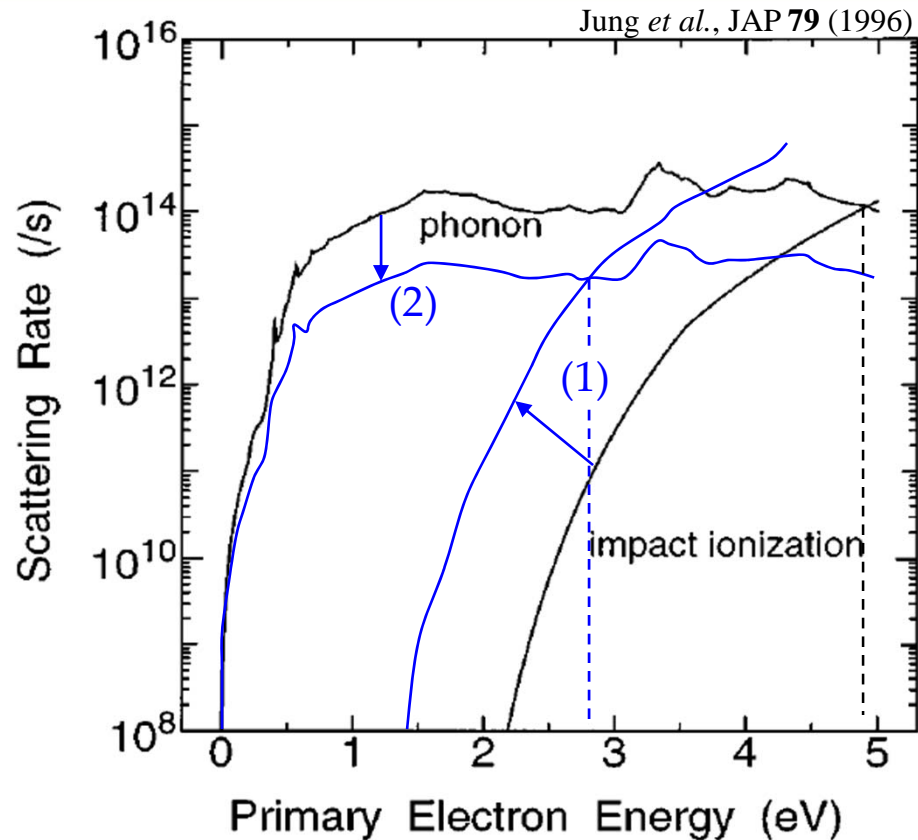
$$\Delta\alpha(t) \propto A_1 \exp(-t/\tau_1) + A_2 \exp(-t/\tau_2) + A_3 \exp(-t/\tau_3) + \dots$$

where the pre - exponential factors  $A_i = \sum_{m=i}^{\infty} P(m)$





# Scattering rates for impact ionization and phonons in bulk GaAs

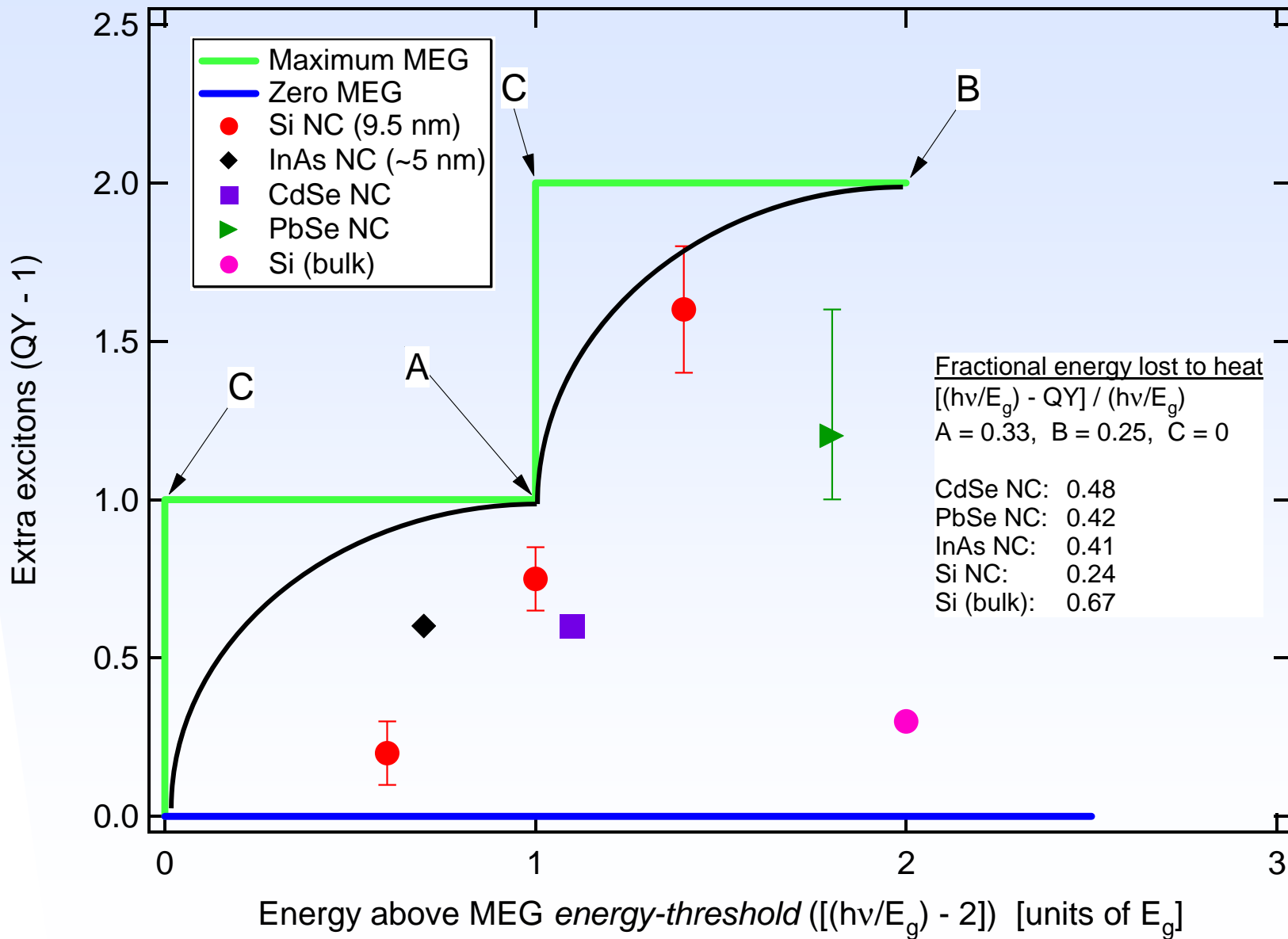


## In NCs:

- (1) Auger processes increase as:  
 $1/(\text{NC dia})^3$ ;
- (2) electron cooling by phonon scattering can be significantly reduced (10X) because of a “partial” phonon bottleneck if Auger cooling can be inhibited.



# How efficiently is excess energy converted to excitons?



Analytical form of intensity-dependent ratio: early/late populations

$$R_{\text{pop}} = \frac{\alpha_{\text{photoinduced}}(t = \tau')}{\alpha_{\text{photoinduced}}(t = \tau'')} = \frac{J_0 \cdot \sigma_p \cdot QY \cdot \delta}{1 - \exp(-J_0 \cdot \sigma_p)}$$

$\tau'$  = short delay (indicates initial exciton density)

$\tau''$  = long delay (indicates fractional exciton population remaining after Auger recombination (max. 1 exciton/NC))

$J_0$  = pump photon fluence (photons  $\cdot$  cm<sup>-2</sup>  $\cdot$  pulse<sup>-1</sup>)

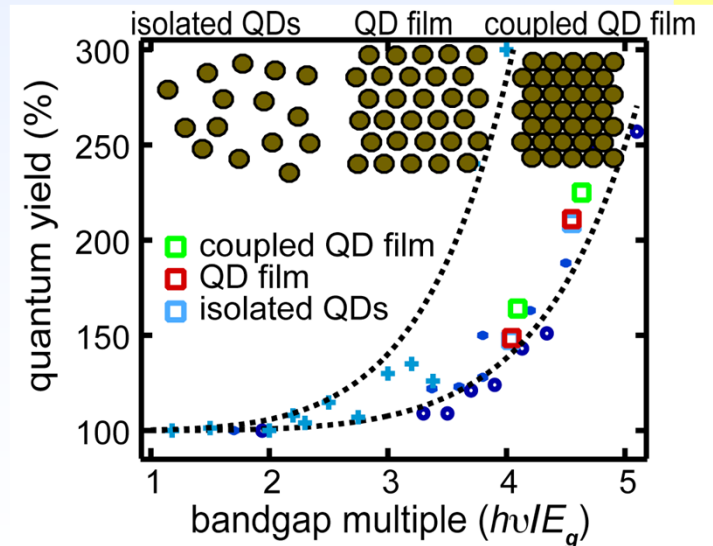
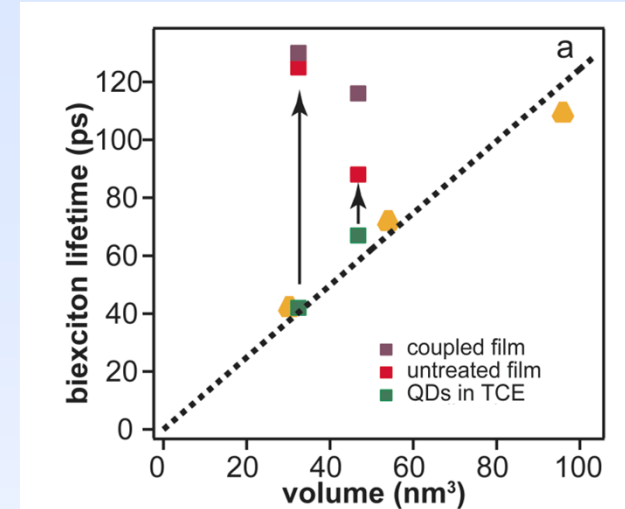
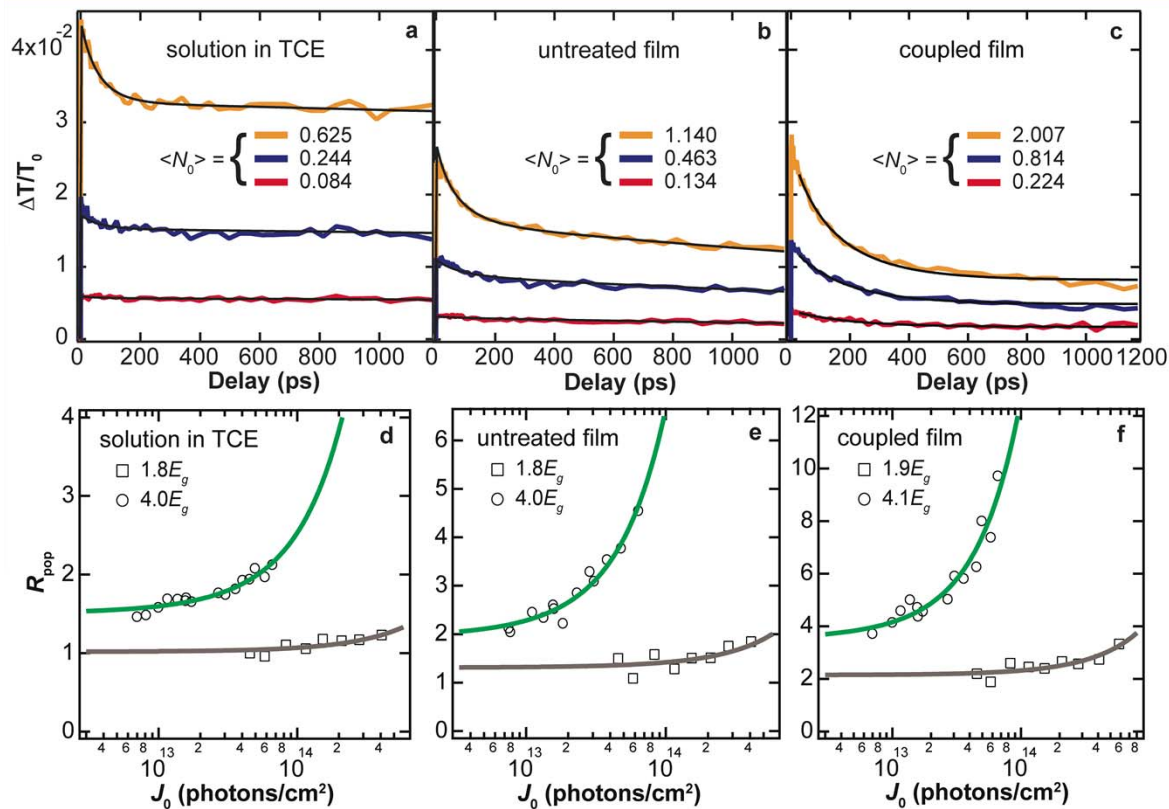
$\sigma_p$  = pump photon energy absorption cross section (cm<sup>2</sup>)

$QY$  = exciton yield (excitons/absorbed photon)

$\delta$  = single exciton fractional decay between  $\tau'$  and  $\tau''$

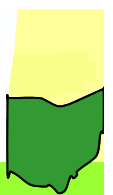


# MEG in arrays of PbSe NCs



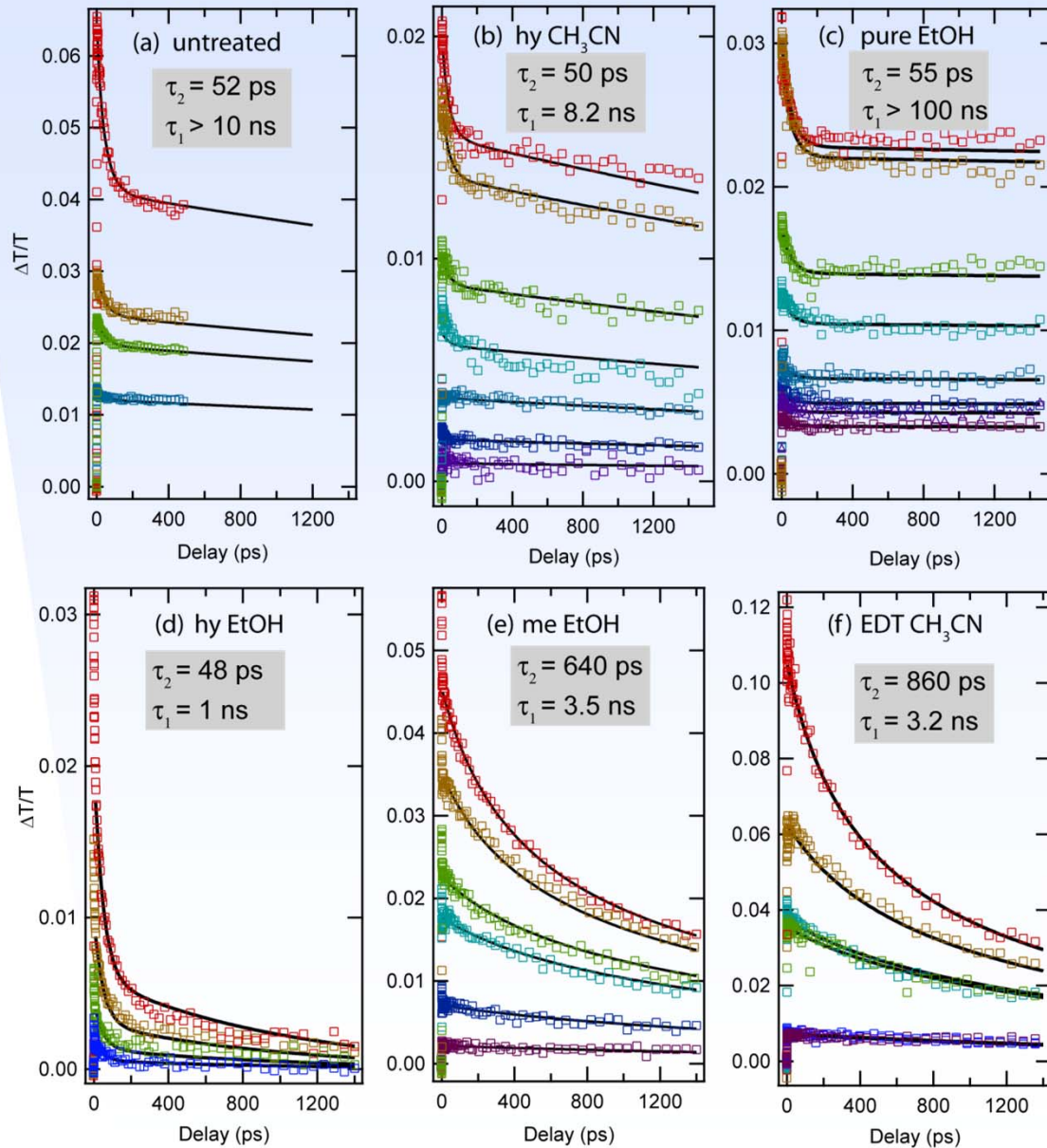
- MEG occurs in these coupled films
- Coupling allows longer time to extract MEG carriers

J. Luther *et al.*, Nano Lett. 7, 1779-1784 (2007).



# PbSe NC films: Biexciton lifetime dependence on chemical treatment

NC size = 3.7 nm

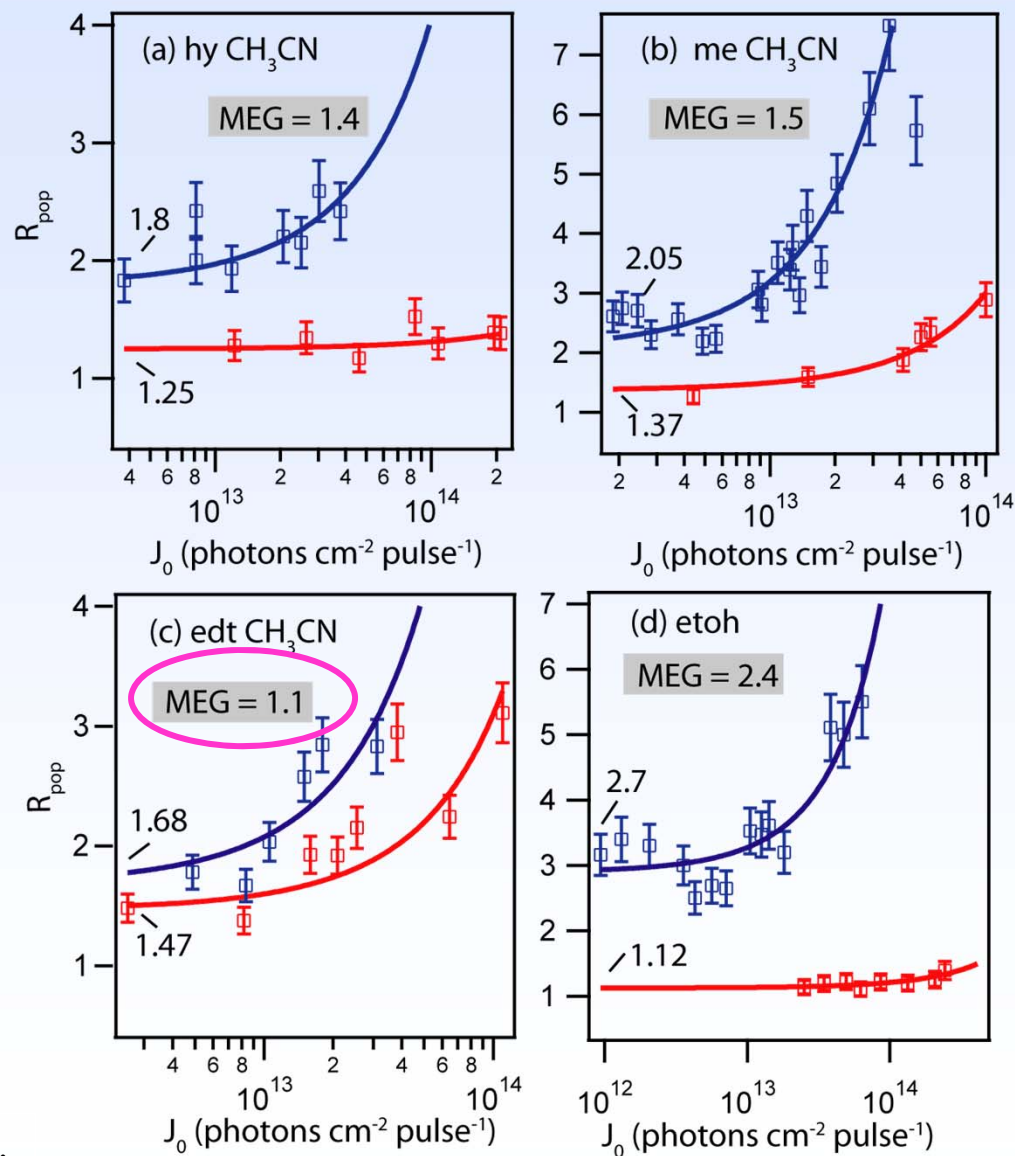


M. C. Beard *et al.*, *Nano Lett.* **2009**, *9* (2), pp 836–845.



# PbSe NC films: MEG QY dependence on chemical treatment

NC size = 3.7 nm



M. C. Beard *et al.*, *Nano Lett.* 9, 836–845 (2009).



## Future directions for NC solar cells

### Opportunities

- low-cost solution-based processing and fabrication techniques
- size-engineered absorption spectra; enhanced IR absorption
- improved efficiency through MEG
- low toxicity NC materials (e.g., Si, Ge)

### Challenges

- efficient charge collection -- record efficiency with semiconductor NCs ~ 3 %
- materials design and development – control of surface/interface properties
- defect tolerance (e.g., Grätzel cell behavior)

Recent MEG review:

Beard, M. C., and Ellingson, R. J., *Laser & Photon. Rev.* **2**, 377-399 (2008).

